International Journal of Biological Macromolecules 242 (2023) 124957

Contents lists available at ScienceDirect

International Journal of Biological Macromolecules

journal homepage: www.elsevier.com/locate/ijbiomac

Mucoadhesive gellan gum-based and carboxymethyl cellulose -based hydrogels containing gemcitabine and papain for bladder cancer treatment

Caroline S.A. de Lima [a,b,*], M. Isabel Rial-Hermida [b,**], Lucas Freitas de Freitas [a], Ana F. Pereira-da-Mota [b], Maria Vivero-Lopez [b], Aryel Heitor Ferreira [a,c], Sławomir Kadłubowski [d], Gustavo H.C. Varca [a], Ademar B. Lugão [a], Carmen Alvarez-Lorenzo [b]

[a] Nuclear and Energy Research Institute, IPEN-CNEN/SP—University of São Paulo, Av. Prof. Lineu Prestes, No. 2242, Cidade Universitária, São Paulo 05508-000, Brazil
[b] Departamento de Farmacología, Farmacia y Tecnología Farmacéutica, I+D Farma (GI-1645), Facultad de Farmacia, Instituto de Materiales (iMATUS) and Health Research Institute of Santiago de Compostela (IDIS), Universidade de Santiago de Compostela, 15782 Santiago de Compostela, Spain
[c] MackGraphe - Mackenzie Institute for Research in Graphene and Nanotechnologies, Mackenzie Presbyterian University, Sao Paulo 01302-907, Brazil
[d] Institute of Applied Radiation Chemistry (IARC), Lodz University of Technology, Wroblewskiego No. 15, 93-590 Lodz, Poland

ARTICLE INFO

Keywords:
Hydrogels
Papain
Polysaccharides
Gemcitabine delivery
Bladder cancer
Permeability enhancement

ABSTRACT

Local treatment of bladder cancer faces several limitations such as short residence time or low permeation through urothelium tissue. The aim of this work was to develop patient-friendly mucoadhesive gel formulations combining gemcitabine and the enzyme papain for improved intravesical chemotherapy delivery. Hydrogels based on two different polysaccharides, gellan gum and sodium carboxymethylcellulose (CMC), were prepared with either native papain or papain nanoparticles (nanopapain) to explore for the first time their use as permeability enhancers through bladder tissue. Gel formulations were characterized regarding enzyme stability, rheological behavior, retention on bladder tissue and bioadhesion, drug release properties, permeation capacity, and biocompatibility. After 90 days of storage, the enzyme loaded in the CMC gels retained up to 83.5 ± 4.9 % of its activity in the absence of the drug, and up to 78.1 ± 5.3 with gemcitabine. The gels were mucoadhesive and the enzyme papain showed mucolytic action, which resulted in resistance against washing off from the urothelium and enhanced permeability of gemcitabine in the *ex vivo* tissue diffusion tests. Native papain shortened lag-time tissue penetration to 0.6 h and enhanced 2-fold drug permeability All formulations demonstrated pseudoplastic behavior and no irritability. Overall, the developed formulations have potential as an upgraded alternative to intravesical therapy for bladder cancer treatment.

1. Introduction

There are approximately 430,000 new cases of bladder cancer (BC) and 165,000 deaths per year around the world due to this pathology. In the first diagnosis of BC, about 30 % of patients have the invasive muscle form of the disease, and among those with superficial tumors, 10–15 % of patients develop the most aggressive form of the carcinoma [1,2]. The treatment of bladder cancer is generally performed by a transurethral resection for the scraping of the visible tumor, followed by adequate therapy according to the stage of the disease [3]. Currently, the instillation of immunotherapy using Bacillus Calmette Guérin is considered the best option for the treatment of high-risk non-invasive cancer [4]. This bacillus stimulates the immune system by inducing cytokine expression through Toll-like Receptors (TLRs) 2 and 4 [5]. However, the success of this therapy is constrained by the difficulties to predict the immune and anti-tumoral responses. Some adverse effects and intolerances could affect 66 % of patients and can even result in severe complications [6]. Moreover, the instillation of pharmaceuticals in the

* Correspondence to: C. S. A de Lima, Nuclear and Energy Research Institute, IPEN-CNEN/SP—University of São Paulo, Av. Prof. Lineu Prestes, No. 2242, Cidade Universitária, São Paulo 05508-000, Brazil.
** Correspondence to: M.I. Rial-Hermida, Departamento de Farmacología, Farmacia y Tecnología Farmacéutica, I+D Farma (GI-1645), Facultad de Farmacia, Instituto de Materiales (IMATUS) and Health Research Institute of Santiago de Compostela (IDIS), Universidade de Santiago de Compostela, 15782 Santiago de Compostela, Spain.
E-mail addresses: caroline.lima@usp.br (C.S.A. de Lima), mariaisabel.rial@usc.es (M.I. Rial-Hermida).

https://doi.org/10.1016/j.ijbiomac.2023.124957
Received 8 February 2023; Received in revised form 27 April 2023; Accepted 16 May 2023
Available online 20 May 2023

human bladder requires the permeation of the active substance through the urothelium, which is a poorly irrigated and highly impermeable tissue. The residence time of a drug in contact with the epithelium is short due to the dilution and washing-out effect of the urine that ends up eliminating it completely. Non-compliance is also a common issue since intravesical therapy requires one instillation per week in the first month, every 15 days in the second month, and once per month until the completion of one year of therapy [7].

Intense efforts are being made for the development of new drug delivery systems that can improve intravesical therapy efficacy. Gel-based microemulsions have been shown to enhance chemotherapy permeation while minimizing drug-triggered irritation of the bladder tissue, suggesting a reduction of possible side effects compared to drug solutions [8]. Poloxamer 407 floating system for intravesical delivery of gemcitabine was demonstrated useful for a 6-h release of gemcitabine avoiding the risk of obstruction of the urinary tract [9]. Liposomes embedded in a thermosensitive gel have also been investigated for the delivery of liposoluble drugs, such as rapamycin. The liposomes released from the gel matrix during 12 h were expected to get in intimate contact with biological membranes and facilitate drug permeation [10]. A triple-therapy strategy for bladder cancer treatment consisted of a gel platform containing gold nanorods for photothermal therapy and iron oxide nanoparticles for induction of ferroptosis and also repolarization of immune-suppressive M2-like phenotype into antitumor M1-like phenotype, stimulating the immune system [11].

Despite the advances, most studies continue reporting limitations in the control of drug release and drawbacks regarding the complexity of the formulations and their cost. Therefore, a patient-friendly effective treatment of bladder cancer is still an unmet clinical need [12].

Mucoadhesiveness has been applied in the pharmaceutical field for >50 years as a strategy to increase the residence time of the drug on the application site and to provide site-specific delivery [13]. Hydrogels containing polymers with hydrogen bond-forming groups (such as -OH and -COOH), ionic charges, flexible chains, and/or adequate surface tension favoring spreading in the mucosa are good candidates for mucoadhesive formulations [14]. In this regard, natural polymers are widely applied to the production of hydrogels for medical purposes due to their high availability and properties of interest [15,16]. Recently, researchers put their efforts on the development of formulation that potentially can form covalent bounds with the bladder mucosa. In the case of chitosan, their cationic nature is an important feature for the adhesion of mucosa. In order to improve this characteristic, thiolated-chitosan nanoparticles were developed for the improvement of mucoadhesive properties increasing the residence time if compared with pristine chitosan formulations [17]. The adhesion of these nanoparticles demonstrated 14-fold higher mucoadhesion than chitosan nanoparticles. Also, methacrylated derivates had been investigated with similar results [18]. In a parallel approach, Kaldybekov et al. [19] developed maleimide-functionalised poly(lactide-*co*-glycolide)-*block*-poly(ethylene glycol) nanoparticles with an improved retention in a lamb urinary bladder mucosa model, when was compared with the results obtained from maleimide-free nanoparticles.

Gellan gum is a natural linear polysaccharide produced by *Sphingomonas elodea* bacteria, composed of units of α-L-rhamnose, β-D-glucose, and β-D-glucuronate in molar ratios of 1:2:1. Gellan gum is biodegradable and mucoadhesive and shows gelation capacity upon exposure to the physiological concentration of cations [20]. Its gelation may be triggered by the presence of ions, temperature and pH. High temperatures cause the polymer chains to be disordered, while lower temperatures (under 50 °C) induce the formation of double helix stabilized by hydrogen bonds. In the presence of cations, these helixes may associate and become a 3-D network. Acid pHs may also trigger the formation of gellan gum gel. Therefore, the acidity and cations containing features of urine would be suitable to provoke physic crosslinking of this polymer [21,22]. Sodium carboxymethylcellulose CMC) is an anionic mucoadhesive cellulose derivative, often used as an excipient for drug formulations and that has also been explored for bladder applications [23,24]. Bivalent positive ions present in the urine have been shown to decrease the mucoadhesion strength of microparticles prepared with CMC, chitosan, and hydroxypropyl cellulose in *ex vivo* experiments. In the particular case of CMC, an increase in sodium ions (up to 0.4 mol/L) did not alter the mucoadhesion to urothelium, but calcium and magnesium attenuated the binding of the polysaccharide [18]. Therefore, the application of the formulation when the urinary bladder is empty may be beneficial. Compared to other mucoadhesive polymers such as chitosan or polycarbophil, the coating of pipemidic acid-loaded Eudragit RS microspheres with CMC was demonstrated able to sustain more the release process once adhered to damaged vesical mucosa [25]. Recently, CMC-functionalized graphene nanoparticles have shown good stability under a wide range of pH values and mucoadhesion capability to the urinary bladder, allowing for retention during at least 20 urinary voidings [24]. Also, a retrospective study on patients that underwent transurethral surgery of bladder tumor revealed that instillation of hyaluronic acid/CMC dispersion decreased the occurrence of urethral stricture 12 weeks after surgery compared to patients without treatment [26].

Proteases are a common chosen strategy to enhance permeation through mucus as proteolytic enzymes can decrease elastic properties and dynamic viscosity of mucin by affecting its three-dimensional mesh structure. Their capacity of cleaving amine bonds within amino acid sequences of mucus glycoproteins is very selective. However, their use is limited by their low stability in unusual environments, *e.g.*, environments where they are not naturally found such as urine. The risk of denaturation due to temperature and pH changes as well as to the presence of other components in a formulation impacts the biological activity of enzymes over a relatively short period [27–29]. Therefore, parameters such as pH and cleavage sites must be considered when choosing a protease as an enhancement permeation agent. Papain is a thiol enzyme, with an optimum pH range between 5.5 and 7.5 [30,31], that presents broad specificity for peptide bonds [32]. It is applied in the pharmaceutical field for the debridement of skin wounds [33,34] and as a permeation enhancer [31]. Some reports on toxic effects and allergenic reactions have led to a restriction imposed by the FDA regarding the use of papain and papain-derived products for topical use [35] which reinforces the need for properly designed formulations for enzyme delivery.

The development of enzyme nanoparticles represents an alternative to overcome such problems [36]. For instance, papain nanoparticles previously prepared by Varca and coworkers [37–39] were hypothesized to have better biopharmaceutical properties—such as cell-specific targeting and improved drug loading capacity—than their bulk counterparts and may be a possible solution for cosmetic or pharmaceutical formulations. These nanoparticles were synthesized using radiation technology to induce crosslinking through disulfide bridges and bityrosines, while preserving biological properties. The nanoparticles size is given by changes in the enzyme assembly after desolvation and irradiation, which is fixed by intramolecular crosslinks [40].

The hypothesis of the present work is that gels prepared with either CMC or gellan gum may enhance the permeability of a chemotherapeutic agent through the bladder tissue by endowing the formulation with mucoadhesive properties and by preserving the activity of a proteolytic enzyme (papain or nanopapain). The aim was to develop improved formulations for intravesical chemotherapy able to enhance the residence time and the permeation capacity of gemcitabine, which is a water-soluble pyrimidine analog that presents high antitumor activity. The clinical outcomes of gemcitabine intravesical therapy of superficial bladder cancer were shown to be strongly dependent on the direct contact between the drug and cancer cells, suggesting that longer periods of exposure would help to improve its efficacy [41]. To carry out the work two types of gels, one based on CMC and the other on gellan gum, were prepared and then evaluated concerning their stability, rheological behavior, retention on bladder tissue and bioadhesion, drug

release properties, permeation capacity, and biocompatibility.

2. Experimental section

2.1. Materials

Gellan gum high acyl (Mw 1,000–2,000 kDa, Kelcogel®) was kindly donated by CP Kelco (Atlanta, USA) and carboxymethylcellulose sodium (Mw 7,500–8,900 KDa, degree of substitution 0.6–0.9) was purchased from Synth (Diadema, Brazil). Poly(vinyl alcohol) 98 % hydrolyzed (Mw 85,000–124,000 Da) was Selvol™ from Sekisui Chemical (Tokyo, Japan). Papain 30.000 USP-U/mg (EC 3.4.22.2), dimethyl sulfoxide, and acetonitrile (HPLC grade) were purchased from Merck (Darmstadt, Germany), Gemcitabine hydrochloride and L-cysteine hydrochloride monohydrate were purchased from Acros Organics (Geel, Belgium); sodium hydroxide (NaOH), monosodium phosphate (NaH_2PO_4), disodium phosphate (Na_2HPO_4), monosodium phosphate (NaH_2PO_4), monobasic potassium phosphate (KH_2PO_4) from Scharlau (Barcelona, Spain); mucin type II (from porcine stomach), ethylenediaminetetraacetic acid (EDTA) sodium fluorescein, acetic acid ($C_2H_4O_2$), and Nα-benzoyl-DL-arginine-p-nitroanilide hydrochloride from Sigma-Aldrich (St Louis, MO, USA). HUVEC (human endothelial, ATCC CRL-1730) and V79 (fibroblasts, ATCC CCL-93) cell lines were used. Culture media used were RPMI (Roswell Park Memorial Institute medium, Sigma-Aldrich, St Louis, MO, USA) and DMEM (Dulbecco's Modified Eagle's Medium, Sigma Aldrich, St Louis, USA) supplemented with fetal bovine serum (FBS, Sigma-Aldrich, St Louis, MO, USA). All other reagents were used in analytical degree.

2.2. Nanopapain synthesis

Nanopapain was synthesized according to a previously described method [39,40]. In an ice bath, papain (10 mg/mL) solution in phosphate buffer (50 mM): ethanol 80:20 (*v*/v) mixture was exposed to γ-radiation from a ^{60}Co source at 10 kGy, with a dose rate of 3.5 kGy h^{-1}. Nanopapain was prepared in the Institute of Applied Radiation Chemistry (IARC), in Lodz University of Technology (Poland).

2.3. Formulations preparation

Two different hydrogels were prepared using a combination of CMC and PVA or just gellan gum as main structural component as summarized in Table 1. Furthermore, two different forms of papain were tested for comparison: native papain and nanoparticulated papain (nanopapain).

To prepare the gellan gum hydrogels, 0.9 % NaCl solution was heated in an oil bath at 100 °C and the polymer was added under magnetic stirring. After complete solubilization of the polymer, the temperature was cooled down and the volume adjusted. The gel was kept in the refrigerator (4 °C) for later use. The CMC gels were prepared by mixing a 1 % stock aqueous solution of PVA (prepared in an autoclave AES-12, Raypa – 20 min cycle, 120 °C) with the CMC solubilized in water by mechanical stirring. After homogenization, glycerin was added and manually mixed until complete uniformization.

Native papain and nanopapain were previously solubilized in 50 mM phosphate buffer (1.71 g/L of monosodium phosphate and 5.07 g/L of di-sodium phosphate, pH 7.4) at a concentration of 10 mg/mL and then added to the gels to reach the concentration of 0.2 % (m/v). For the formulations containing gemcitabine, the drug was first added to the papain solution or buffer (for controls, C1 and G1) and vortexed until solubilization before the addition to the gels.

2.4. Stability assay

The stability of all formulations was evaluated under storage at refrigerated conditions (4 °C) for 90 days. Firstly, the gels (gellan and CMC + PVA) were autoclaved (20 min cycle, 120 °C in an AES-12 equipment, Raypa) for sterilization. To avoid oxidation, the CMC + PVA blend was autoclaved separatedly from the glycerin and then mixed under laminar flux in a biological safety cabinet. The papain and the gemcitabine solutions were filtered (PTFE hydrophilic, Syringe Filter, 0.22 μm 13 mm; Scharlab S.L., Spain) and added to the formulations under sterile conditions. The gels were aliquoted into 2 mL glass vials, without headspace to minimize the presence of oxygen and, consequently, papain oxidation. The flasks were maintained in a refrigerator (4 ± 2 °C), sheltered from light, and evaluated concerning their visual aspect, pH, and proteolytic activity of the papain (for those formulations containing enzyme) after 0, 15, 30, 60, and 90 days.

Papain proteolytic activity was evaluated according to the method described by Ferraz and coauthors [42]. Briefly, a 5 % (*w*/*v*) solution of the formulations in 50 mM phosphate buffer was prepared in order to decrease the viscosity and enable the reaction. In a 96 well plate, 100 μL of the diluted formulations were pipetted together with 120 μL of Nα-Benzoyl-DL-arginine p-nitroanilide hydrochloride previously diluted into a cysteine-versene buffer (0.8 mg/mL). The plate was maintained at 40 °C and after 0, 15, 30, and 45 min, the reactions were stopped by pipetting 50 μL of acetic acid (10 % *v*/v). In a plate reader spectrophotometer (BIORAD Model 680 Microplate Reader, USA), the absorbance was assessed at 415 nm [42]. The activity of the enzyme was estimated from the slope of the increase in absorbance *versus* time. On time zero,

Table 1
Composition of the formulations.

CMC + PVA Formulations							
Code	CMC (m/v)	PVA (m/m)	Glycerin (v/v)	H_2O (v/v)	Native papain (m/v)	Nanopapain (m/v)	Gemcitabine (m/v)
C	2.0 %	0.2 %	20.0 %	77.8 %			
C1	2.00	0.2 %	20.0 %	76.8 %			1 %
C2	2.0 %	0.2 %	20.0 %	77.6 %	0.2 %		
C3	2.0 %	0.2 %	20.0 %	76.6 %	0.2 %		1 %
C4	2.0 %	0.2 %	20.0 %	77.6 %		0.2 %	
C5	2.0 %	0.2 %	20.0 %	76.6 %		0.2 %	1 %

Gellan Gum Formulations					
Code	Gellan Gum (m/v)	NaCl 0.9 % solution	Native papain (m/v)	Nanopapain (m/v)	Gemcitabine (m/v)
G	0.1 %	99.9 %			
G1	0.1 %	98.9 %			1 %
G2	0.1 %	99.7 %	0.2 %		
G3	0.1 %	98.7 %	0.2 %		1 %
G4	0.1 %	99.7 %		0.2 %	
G5	0.1 %	98.7 %		0.2 %	1 %

activities were compared to controls of native papain and nanopapain without the presence of the gels. For evaluation through time (30, 60, and 90 days), the initial proteolytic activity found at time 0 was considered 100 %. All the formulations were evaluated in triplicate.

2.5. Fourier transform infrared spectroscopy

To perform FTIR analysis, formulations were previously lyophilized. A Vertex 70v (Bruker, Billerica, MA, USA) equipment was used, at 18 °C with 2 cm^{-1} of resolution, from 400 to 4000 cm^{-1}.

2.6. Differential scanning calorimetry (DSC)

DSC was done in a Mettler Toledo/822 (USA) equipment, with 8 mg of each formulation, previously lyophilized, in a temperature range varying from −30 °C to 220 °C (10 °C/min) in nitrogen atmosphere (50 mL/min).

2.7. Rheological measurements

The rheological behavior of the formulations was evaluated in a Physica MRC 301 (Anton Paar, Austria) rotational rheometer, with plate-plate geometry (gap of 1 mm). First, formulations were tested concerning amplitude sweep (0.1–100 %) and frequency sweep (ω = 25–150 rad/s for gellan gum and ω = 0.1–100 rad/s for CMC + PVA). Then, the formulations viscosity was analyzed under shear rate variation. All assays were performed at 37 °C, before and after the addition of papain.

2.8. Formulations interaction with mucin

The interaction between the hydrogels and the mucin present in the urothelium bladder was evaluated using an AR 1000-N rheometer (TA Instruments, USA). To carry out the test, a mucin stock solution was freshly prepared in the day of the experiment, by mixing 1 g of mucin type II with 9 g of ultrapure water and left under magnetic stirring until complete homogenization. One-part of this 10 % (*w*/w) mucin solution and one-part of hydrogel were mixed and stirred vigorously for 2 h before analysis. Then, the measurements were performed in triplicate. The temperature was set to 37 °C, and viscosity was assessed under shear rates varying from 1 to 200 s^{-1} [43]. Controls were prepared by mixing the gels with deionized water.

2.9. Hydrogels retention on bladder tissue

Hydrogel retention on *ex vivo* bladder tissue was carried out according to the methodology described by Kolawole et al. [16] with some modifications. Fresh porcine bladders were obtained from a local slaughterhouse (Frigorífico Suzano, Suzano, Brazil) and transported under refrigeration. The bladders were opened and slices of approximately 2 × 2 cm were cut, avoiding contact and pressure on the urothelium in order to preserve its structure. The tissue slices were then rinsed with 3 mL of artificial urine (pH 6.2) [44] and 50 μL of each formulation previously dyed with sodium fluorescein (0.1 %) were applied over the urothelium. After 10 min, 5 washing cycles with 5 mL of artificial urine were performed for each tissue piece. Artificial urine was prepared according to a protocol described previously [44]. In the intervals between the washes, the tissues were evaluated in a fluorescence microscope (Nikon 80i, Tokyo, Japan). The experiment was done in triplicate and sodium fluoresceine in phosphate buffer was used as control. Images obtained were analyzed using Image J software to evaluate fluorescence intensity of samples, indicating, mucosa retention quantitatively.

2.10. Bioadhesion strength

Fresh porcine bladders were obtained from Compostelana de Carnes slaughterhouse (Santiago de Compostela, Spain). To measure the adhesion strength of the hydrogels to the urothelium, bladder fragments of 2 × 2 cm each were placed in a TXT Plus Texture Analyzer (Stable Micro Systems, UK). One of them was attached to the geometry and the other placed on the lower platform inside a Petri dish, in a way that the two fragments were arranged with their respective urothelium "face to face". Then, 800 μL of each hydrogel formulation were placed on the fragment fixed to the lower platform of the texturometer, and the equipment was programmed so that the upper tissue (without formulation) came in contact with the lower one for 1 min. After this period, the equipment separated the two fragments and registered the total detachment force and the adhesion work. The equipment was programmed with the following parameters: pre-speed test 1 mm/s; test speed 1 mm/s; post-test speed 1 mm/s; applied force 0.5 N; contact time 60 s; trigger force 0.0009 N; return distance 15.0 mm. A graph of the strength by distance was generated for each analysis. The maximum force to detach the urothelium from the hydrogel indicated the adhesive strength of the formulation, and the total adhesion work was evaluated through the area under the curve of the force-distance graph [16,45].

2.11. In vitro drug release

The *in vitro* release studies were carried out in triplicate by placing dialysis bags (MWCO = 1000 Da) containing 1 mL of each formulation into plastic vials with 30 mL of saline buffer at 37 °C and 100 rpm. At pre-set times (0, 0.5, 1, 2, 4, 6, 8 h and 1, 2, 3, 4, 5, 6, and 7 days) aliquots of 1 mL were collected from the release medium and replaced with the same volume of fresh medium. The amount of drug released was quantified by HPLC using a previously validated calibration curve in the same medium. The calibration curve was between 0.5 ppm and 50 ppm, with accuracy of 98.7 %, precision with coefficient of variation <3 %, and linearity with CVFR <5 %. The HPLC analysis was carried out using a 50 mM phosphate buffer containing 0.660 g of heptanosulfonate as ion pairing (pH = 3) and acetonitrile (90:10) mobile phase (1 mL/min) through a Spherisorb ODS2 column (5 μm, 4.6 mm × 250 mm), at 40 °C and a run time of 10 min (retention time of approx. 5 min). The injection volume was 80 μL and the UV detector was fixed at 268 nm [46].

2.12. Ex-vivo drug permeation

The permeability capacity of the most promising formulations was evaluated *ex vivo* in triplicate following a previously described protocol with slight modifications [47]. Fresh porcine bladder pieces (0.785 cm^2) from a local slaughterhouse (Compostelana de Carnes, Santiago de Compostela, Spain) were placed in Franz cells with receptor and donor chambers filled with 6 and 2 mL of PBS (pH 7.4) respectively. The receptor compartment was kept at 37 ± 2 °C and 100 rpm. Several pieces of the same bladder were used for the test of all formulations in order to minimize tissue-dependent deviation. After 30 min, the whole quantity of PBS in the donor chamber was removed with a Pasteur pipette and replaced for 2 mL of the hydrogel formulations containing gemcitabine ($n = 3$). At pre-determined times (0.5, 1, 2, 4, 6, and 7 h), 1 mL aliquot was removed from the receptor chamber and replaced with fresh PBS. Aliquots were frozen at −20 °C until being analyzed by HPLC as described above. After 7 h, the donor chamber content was removed, and the bladder tissues were transferred to tubes containing 3 mL of a 50 % DMSO (*v*/v) solution for gemcitabine extraction. The tubes containing the tissues were transferred to a mini shaker (Heidolph, Schwabach, Germany) and kept at 37 °C and 100 rpm for 24 h. Then, the tubes were centrifuged for 5 min and 1000 rpm, under 25 °C. The supernatant was filtered, centrifuged again for 20 min at 14,000 rpm and used for later HPLC quantification. The gemcitabine steady state flow (J) of each formulation tested was calculated from the slope of the linear regression

obtained from the concentration of drug in the receptor chamber *versus* time, and the lag time (T_0) by its intersection of the x-axis [48].

2.13. Biocompatibility evaluation: cytotoxicity and HET-CAM assays

HUVEC (human endothelial ATCC CRL-1730) and V79-4 (fibroblasts, ATCC CCL-93) cell lines were used for the cell compatibility assays. In a 96-well plate, 5×10^3 cells were seeded in each well, containing 100 μL of culture medium. After 24 h of incubation in an oven at 37 °C with a humid atmosphere of 5 % CO_2, the culture medium was removed and replaced with a mixture of 50 % of culture medium and 50 % of each gel, with or without native or nanoparticulate papain. Native and nanoparticulate papain in buffer, at the same concentration as in the gels, were also tested. The cells were incubated at 37 °C with a humidified atmosphere of 5 % CO_2 for 24 h. After this period, 25 μL of MTT solution were added to each well, and the plates were incubated again for 3 h. After this period, 100 μL of DMSO was added to solubilize the MTT metabolized by the viable cells and the plates were read in an ELISA reader (Spectramax i3), using a wavelength of 550 nm. Formulations results were compared with negative controls (cells incubated with culture medium containing PBS instead of hydrogel). Each formulation, including controls, was tested in 4 wells of the plate. The data averages of each group of wells were compared with negative control using one-way ANOVA, considering $p < 0.05$.

The HET-CAM test (hen's egg-chorioallantoic membrane test) was carried out using fertilized hen eggs (50–60 g each egg donated by Coren, Spain) that were incubated at 37 °C and 60 % relative humidity (Ineltec climatized chamber, CC SR 0150, Barcelona, Spain) for 8 days. The eggs were rotated every day to avoid sticking the embryo to one side of the shell. On the eighth day, the CAM was exposed after removing the upper part of the eggshell with a needle and the inner membrane after wetting it with 0.9 % NaCl solution. Then, 300 μL of each formulation were placed in contact with the CAM for 5 min and the time at which hemorrhage (H_{time}), lysis (L_{time}), and/or coagulation (C_{time}) started was registered to calculate the irritation scores (IS) using Eq. (1). Negative (0.9 % NaCl) and positive (0.1 N NaOH) controls were tested in the same way [49].

$$IS = \left(\left(301 - \frac{Htime}{300}\right)*5\right) + \left(\left(\frac{301 - Ltime}{300}\right)*7\right) + \left(\left(301 - \frac{Ctime}{300}\right)*9\right) \quad (1)$$

According to IS values, materials could be non-irritating (0.0–0.9), weakly (1–4.9), moderately (5–8.9), or severe (9–21) irritating. The assay was performed in duplicate [49].

2.14. Statistical analysis

The results were expressed by means ± standard deviation. Statistical significance ($P < 0.05$) was determined for relative activity of papain after being added to the gels, mucoadhesion strength and cytotoxicity assays using one-way ANOVA (GraphPad Prism software; La Jolla, CA, USA). Permeation and fluorescence intensity statistical significance were obtained by two-way ANOVA (GraphPad Prism software; La Jolla, CA, USA).

3. Results and discussion

3.1. Formulations preparation and stability

As described in the introduction, the use of polysaccharides as biocompatible and mucoadhesive polymers is being incipiently tested in the localized therapy of bladder cancer. Gellan gum and CMC have the additional advantage of *in situ* gelling due to the presence of divalent positive ions in urine [20,50]. Mixtures of CMC with PVA have been widely explored in the pharmaceutical field because they form an interpenetrating network driven by hydrogen bonds that lead to synergic mechanical reinforcing properties [51,52]. Glycerin was added to the blend to increase plasticity and act as a preservative. The gel compositions were kept as simple as possible to explore their capability to act as a vehicle for papain and gemcitabine. The proteolytic enzyme papain was proposed, for the first time, as a permeation enhancer agent for superficial bladder cancer therapy. Thus, enzyme stability represented an additional aim. It was foreseen that the gels could present good adhesion to the urothelium, enhancing residence time and penetration of gemcitabine, while slowing down the drug release and diminishing side effects of the therapy.

All formulation components showed good miscibility and the as prepared hydrogels presented homogeneous visual aspects and viscosity (Fig. S1 in Supplementary Material). The hydrogels were monitored for 90 days regarding visual aspect, pH, and proteolytic activity of papain to evaluate their stability under storage at 4 °C and protected from light. All hydrogels demonstrated a homogeneous aspect from time zero to day 90, with excellent stability. On the 90th day, all formulations containing gellan gum showed a white precipitate with a completely transparent supernatant, indicating destabilization of the gels. At this point, the CMC + PVA formulations showed a little decrease in the viscosity probably due to the papain amylolytic activity.

The pH of all formulations decreased with the addition of gemcitabine to a range between 3 and 4, and no changes were observed between the initial ($t = 0$ days) and final ($t = 90$ days) time in any formulation (Fig. S2 in Supplementary Material). Papain may lose its tertiary structure below pH 2, beginning the denaturation process. According to a previous study on the effects of pH and temperature on papain stability [53], under the tested storage conditions papain should still present a residual activity above 75 %.

At time 0, the relative activity of papain nanoparticles (nanopapain) was 44.7 ± 1.0 % compared with the native one (Fig. 1a). This was expected considering that the synthesis process by radiolitic means can compromise its activity by up to 30 % [39]. In general, no loss in activity was observed after the incorporation of papain nanoparticles in the polymer gels. All gellan gum formulations maintained at least 90 % of the activity of the native papain or the nanopapain as prepared (Figs. 1b and c). In addition, for the formulation containing gellan gum and nanopapain, without gemcitabine, the enzyme activity was even increased suggesting some synergism between the gel and the protein (Fig. 1c). On the other hand, CMC + PVA native papain formulations (Fig. 1b) presented 81.3 ± 7.3 % and 85.1 ± 9.5 % activity containing or not gemcitabine, when compared to the isolated native enzyme activity. Similarly, CMC + PVA hydrogels with papain nanoparticles (Fig. 1c), presented good activity of 92.7 ± 5.2 %, but the presence of the drug decreased the enzyme activity to 65.9 ± 13.6 %.

The relative activity of the formulations was also evaluated during the 90 days, considering time zero activity as 100 % of activity for each formulation (Fig. 2). A decrease in activity was expected as papain may consume itself in an autolyze process, although the viscosity of the hydrogel matrix in which the enzyme was embedded could have influence in the kinetic of this process [54,55]. After 90 days, the CMC + PVA formulations containing papain and nanopapain presented 83.5 ± 4.9 % and 83.3 ± 0.4 % of residual activity. Sheng and colleagues found that after 28 days under 4 °C storage, native papain lost 50 % of its initial activity as, meanwhile, papain immobilized on porous magnetic nanoparticles lost 15 % in the same period [56]. In the present study, the loss of activity in 90 days for these both formulations were equivalent to the immobilized enzyme in 28 days. The incorporation of the gemcitabine and the consequent decrease in the pH of the CMC + PVA hydrogels caused a decrease in the residual activities, which were 78.1 ± 5.3 % for hydrogel with native papain after 90 days of storage and 35.7 ± 16.6 % for those containing nanopapain after 30 days storage. Differently, gellan gum-based formulations showed a higher decrease in residual activity values after 30 days, but after 90 days, the residual activity of formulations containing native papain was 62.7 ± 22.8 % in the absence

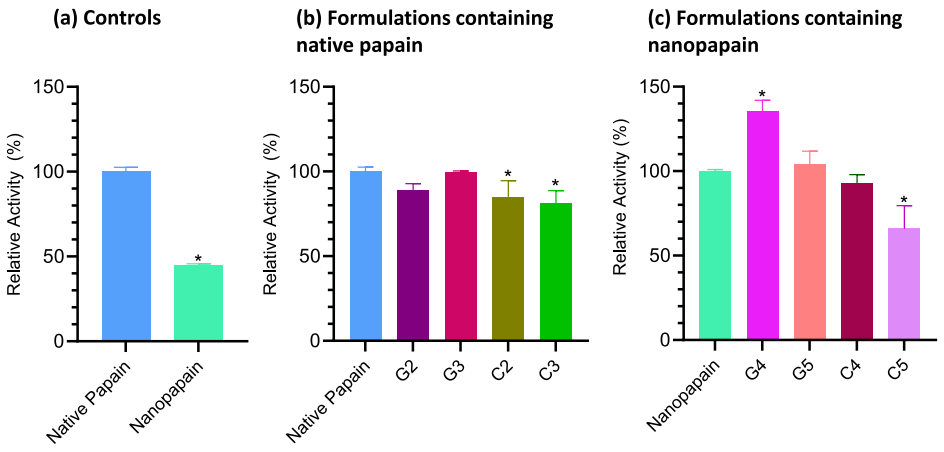

Fig. 1. Enzymatic activity at the beginning of the stability experiment (time = 0 h) of (a) native papain and nanopapain; (b) formulations containing native papain and (c) formulations containing nanopapain. Codes as in Table 1. * indicates statistical significance between control (native or nanopapain isolated) and samples ($p < 0.05$).

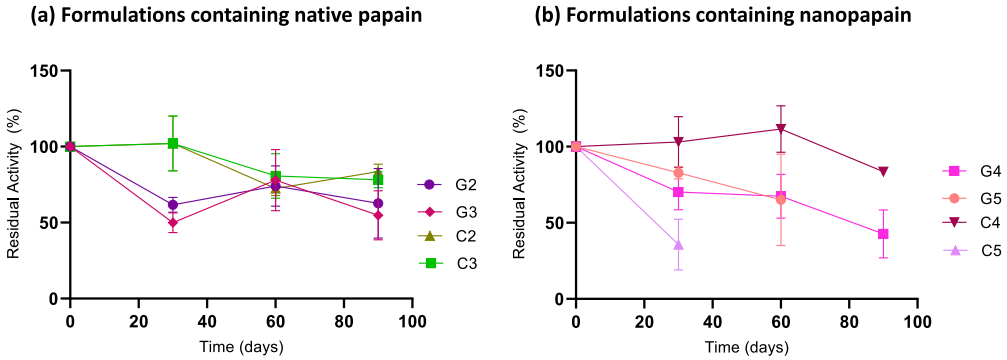

Fig. 2. Residual papain activity during the 90-day storage period at 4 °C for formulations prepared with (a) native papain and (b) nanopapain. Codes as in Table 1.

of gemcitabine and 54.8 ± 16.1 in the presence of the drug. Nanopapain also showed a decrease in activity in the presence of gemcitabine, as observed for CMC + PVA formulations.

Thus, stability studies demonstrated that the developed hydrogels were able to extend papain proteolytic activity up to 90 days. The CMC + PVA blend presented better conditions to preserve the enzyme, which was more stable and functional for a longer period in its native form than the nanoparticulated one. CMC and PVA blends have been used previously for the immobilization of enzymes, including, papain and demonstrated to be a good support for proteolytic activity preservation [57].

3.2. Fourier transform infrared spectroscopy (FTIR)

The FTIR spectra of gellan gum gels (Fig. 3a) were very similar to that of pristine Kelcogel® powder (Fig. S3 in Supplementary Material). At 3400 cm^{-1} a band related to -OH stretching groups present in the glucopyranose rings was observed. A peak related to glycosidic bonds in gellan gum structures was identified at 1618 cm^{-1} [58,59] while a peak at 1723 cm^{-1} showed the presence of acyl groups [60].

CMC powder spectrum (Fig. 3b) displayed a wide but low intensity band at 3300 cm^{-1} related to hydroxyl stretching bonds, at 2920 cm^{-1} a small band related to asymmetric stretching of CH_2 bonds, and at 1600 cm^{-1} a band due to the COO- stretching. In 1420 cm^{-1} a small band related to the scissoring bending of CH_2 was identified, another one in 1330 cm^{-1} due to angular deformation of hydroxyl, and, finally, a band in 1062 cm^{-1} due to CH-O-CH_2 stretching was also observed. PVA spectrum also presented bands similar to the ones described in the literature: 3300 cm^{-1} due to OH stretching; one band with low intensity in 2948 cm^{-1} due to asymmetric stretching of CH_2; a band in 1726 cm^{-1} related to residual C═O stretching of acetate groups from polyvinyl acetate hydrolysis process; in 1084 cm^{-1} a C—O stretching band; and in 840 cm^{-1} another band due to CH_2 twisting mode bond [51]. The lyophilized blend CMC-PVA gel spectrum showed an increased intensity in the band around 3304 cm^{-1} associated to the hydroxyl groups stretching. The band related to PVA carbonyls (1726 cm^{-1}) turned into a small shoulder in 1722 cm^{-1} and CMC carboxylic group (1600 cm^{-1}) shifted to 1672 cm^{-1} with less intensity, indicating both components miscibility. Other changes in bands between 1520 and 800 cm^{-1} were observed due to the mixing process. The band related to PVA crystalline structure in 1084 cm^{-1} became wider, due to the vibration mode of CH-O-CH_2 in 1062 cm^{-1} from CMC molecules. These modifications suggest the formation of intermolecular hydrogen bonds between PVA and CMC, as previously reported [51].

Native papain FTIR results (Fig. 3c) revealed a band related to the hydroxyl stretching (3306 cm^{-1}), followed by a small one in 2935 cm^{-1} related to C—H (sp3) bonds. In 1644 cm^{-1} and 1549 cm^{-1} bands of carbonyl stretching from amides I and II from the protein secondary structure were identified. Deformations in 1043, 1071 and 874 cm^{-1} related to the stretching of C—S bonds were also observed [61,62]. Nanopapain presented a very similar FTIR spectrum, but with less intensity, except for the one at 865 cm^{-1} related to the stretching mode of C—S.

The gemcitabine spectrum (Fig. 3d) presented FTIR bands related to amines N—H stretching (3387 cm^{-1}), to alkenes or aliphatic C—H (2948 cm^{-1}); to C═O (in 1535 cm^{-1}) and C—H also to C—H (718 in cm^{-1}) in aromatic rings [63,64].

The gellam gum gels containing native and nanoparticulated papain

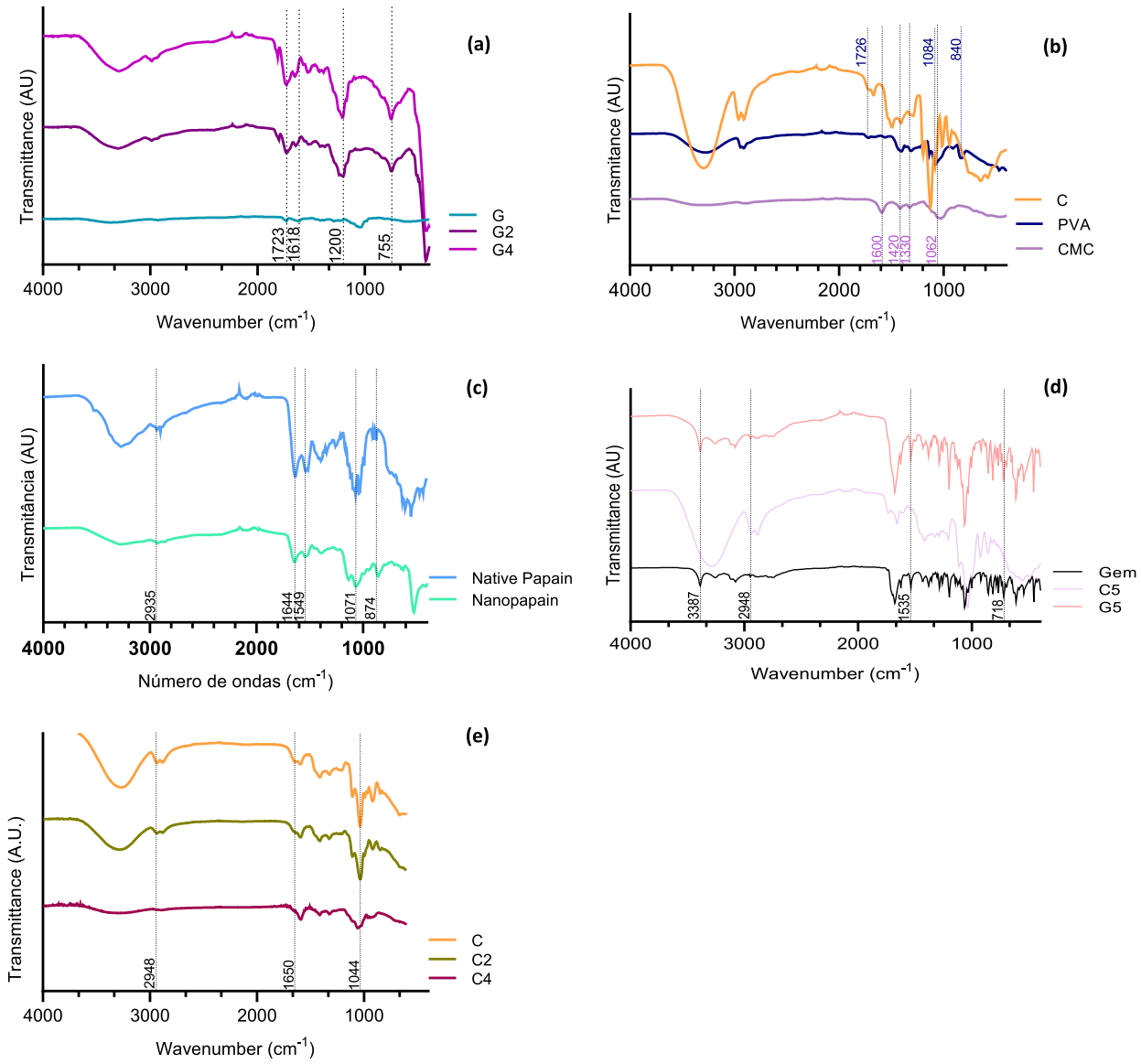

Fig. 3. FTIR spectra of (a) gellan gum formulations; (b) CMC and PVA formulation and raw powders; (c) native papain and nanopapain; (d) formulations containing gemcitabine; (e) CMC + PVA formulations. Codes as in Table 1.

(0.2 % *w/v* – Fig. 3a) did not present changes in their spectrum revealing no chemical interactions between the polymers and the enzyme. When gemcitabine was added to the gels, the formulations presented bands typical of the drug substance as previously described (Fig. 3d).

On the other hand, the addition of nanopapain into the CMC + PVA blend (Fig. 3e) caused a diminution of the intensity of bands at 2948 (CH_2 asymmetric stretching), 1650 and 1044 cm^{-1}. In the presence of gemcitabine and the nanopapain, bands at 1650, 968, and 933 cm^{-1} became more intense, a new band appeared at 1295 cm^{-1} and the band at 1600 cm^{-1} lost intensity. These modifications may suggest interactions between the polymer matrix, the nanoparticles, and the drug, such as new hydrogen bonding and van der Waals interactions.

3.3. Differential scanning calorimetry (DSC)

DSC analysis were carried out to gain further insight into possible interactions between the polymeric matrices, the enzyme and the drug in terms of changes in the first and second order transitions. Native papain and nanopapain (Fig. 4a) showed endothermic peaks at 152.1 °C and 125.2 °C, respectively. These events are related to the enzyme denaturation process, in which there are breaks of N—H bonds and oxygens from adjacent carboxylic groups, causing changes in the 3D structure of the enzyme and impairment of the α-helix [33]. There was a widening of this peak in the analysis of the nanoparticulate papain when compared to the native one probably due to changes in the molecular assembly due to gamma radiation used in the synthesis process. Another issue is the presence of salts in the buffer in which the nanopapain was synthesized, which may influence the thermal transition.

Gemcitabine hydrochloride calorimetric analysis (Fig. 4b) showed an endothermic peak at 282.8 °C related to the fusion of the crystalline drug [63]. Then an exothermic peak appeared due to degradation. Kelcogel® gellan gum had an endothermic peak at 154 °C and another exothermic peak at 247.4 °C (Fig. 4c). The first event was related to the melting process of the crystalline portion of the polymer and the second indicated the beginning of the degradation process [65]. The lyophilized gellan gum gel showed similar peaks (endothermic at 172 °C and exothermic at 242 °C), however with lower enthalpy. Formulations containing native or nanoparticulate papain showed endothermic peaks at temperatures close to the protein melting point.

The CMC + PVA blend (Fig. 4d) showed an endothermic peak at

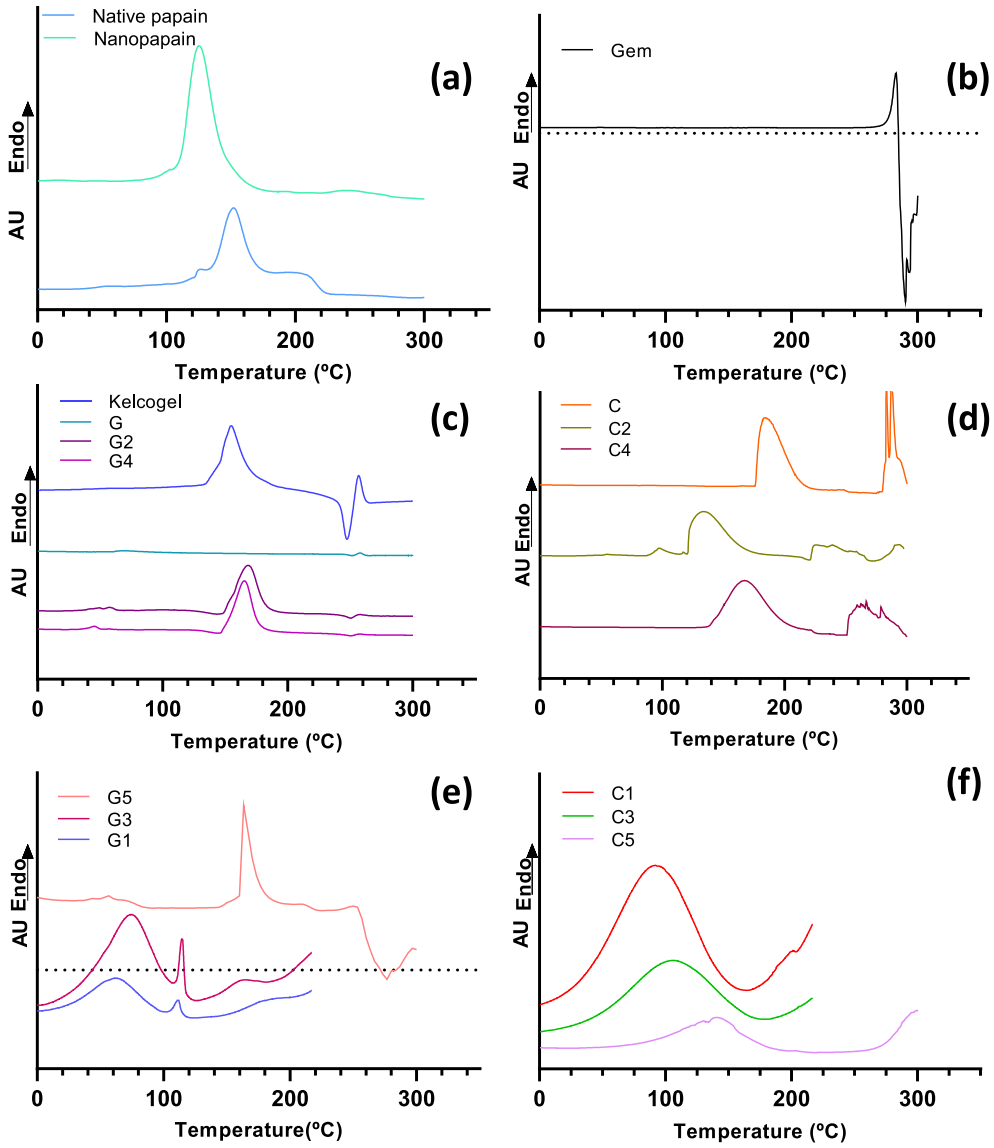

Fig. 4. DSC of lyophilized formulations: (a) nanopapain and native papain (raw); (b) raw gemcitabine; (c) gellan gum hydrogels with and without papain; (d) CMC + PVA hydrogels with and without papain; and (e) gellan gum and (f) CMC + PVA formulations containing gemcitabine. Codes as in Table 1.

183.9 °C referring to the melting of the small crystalline portion of the PVA [66] The presence of papain in both native and nano forms in the blend anticipated the melting process to 133.9 °C and 167 °C, respectively.

Finally, the thermal behavior of gels in the presence of gemcitabine, containing or not papain/nanopapain was also analyzed. In the case of gellan gum formulations (Fig. 4e), the endothermic peaks were recorded at 62.23 and 111.51 °C (G1); 73.65 and 114.9 °C (G3), and 162.7 °C (G5) related to water evaporation, polymer melting and papain denaturation. In the CMC and PVA gels (Fig. 4f), the water evaporation and papain denaturation peaks were also observed at 92.33 °C (C1), 104.88 °C (C3), and 140.0 °C (C5).

3.4. Rheological measurements

Firstly, amplitude sweep tests (Supplementary material- Fig. S4) were performed to identify the stress range in which the viscoelastic behavior of the formulations was linear and that, therefore, the structure of the gels was stable and G' remained constant. [67]. After the linear region, a nonlinear region is usually observed due to the partial collapse of the three-dimensional network of the gel, followed by the intersection of storage modulus (G') and loss modulus (G") and then the predominance of a characteristic liquid behavior [68]. Thus, for gellan gum formulations, viscoelastic strain range was between 1 and 44 %; while for CMC + PVA blend it was 0.01 and 100 %.

In the frequency sweep analysis (Fig. 5 a,b,c) at low frequency, CMC + PVA formulations presented G" higher than G', typical of soft viscous gels. The progressive increase of the frequency caused that the G' became higher than G", and the formulation performed as a solid-like viscoelastic material. On the other hand, gellan gum formulations had G' values higher than G" ones (Fig. 5 d,e,f) for the entire frequency range, meaning that even under low frequencies the formulations performed as well-structured gels.

Analyses evaluating the viscosity in relation to the shear rate were also performed. [68]. The hydrogels showed a decrease in viscosity as the shear rate increased (Fig. 6). Non-Newtonian shear thinning behavior has previously been reported for polysaccharide gels such as gellan and CMC [16,69,70]. The viscosity values at rest are compatible with administration through a syringe while the shear thinning may facilitate the complete delivery of the whole dose with less effort. CMC + PVA gels showed less intense shear-thinning compared to gellan gum gels probably due to the dynamic hydrogel bonding between both

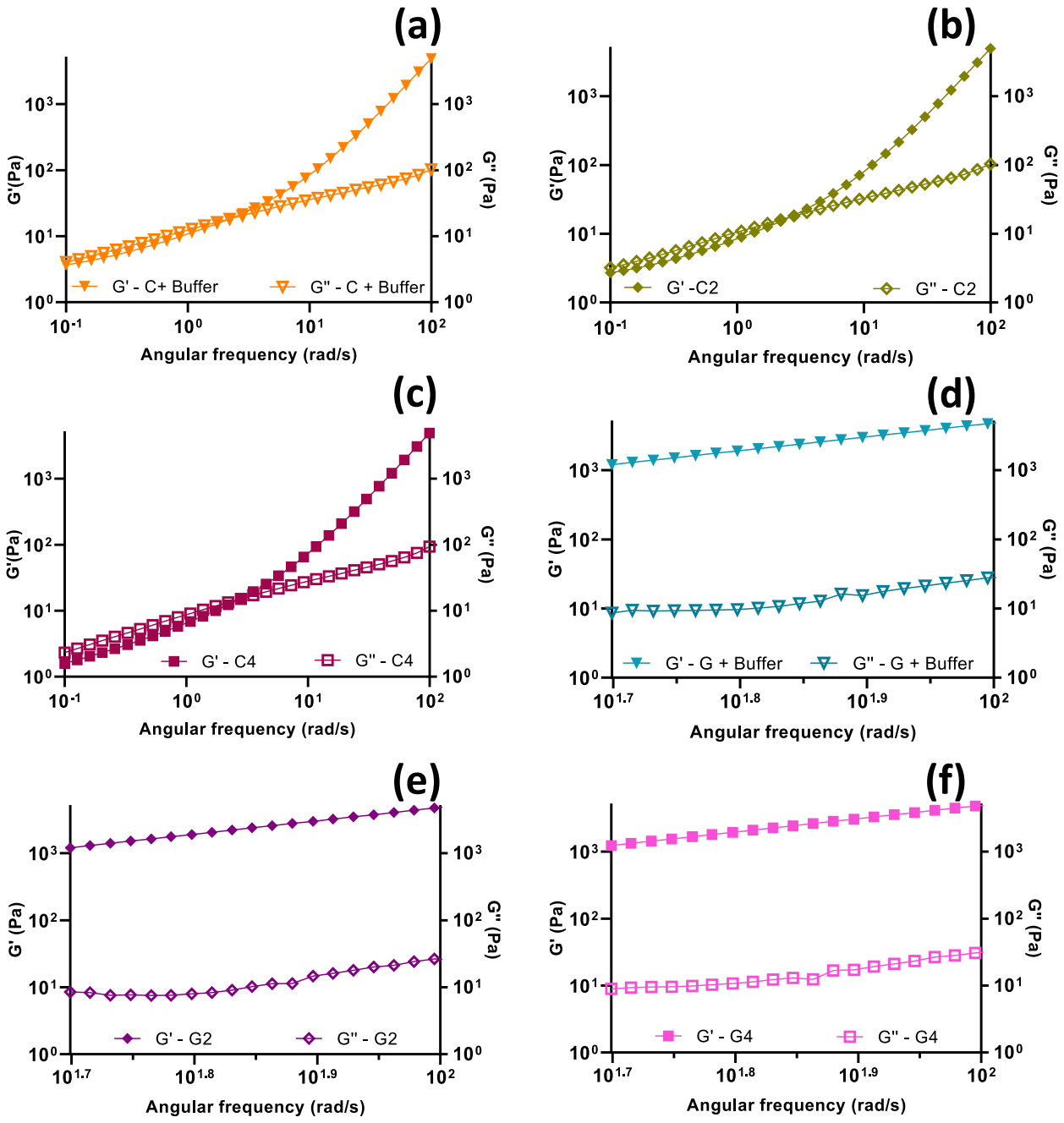

Fig. 5. Frequency sweep of CMC + PVA formulations (a) C, (b) C2, (c) C4; and gellan gum formulations (d) G, (e) G2, and (f) G4 at 37 °C. Codes as in Table 1.

polymers, which allows for fast self-healing under intense stress [71]. Also, compared to gellan gum gels in which the addition of papain had no effect, CMC + PVA gels showed a decrease in the viscosity at rest in the presence of papain, which suggests that the enzyme causes partial hydrolysis of the polymer chains [72].

3.5. Formulations interaction with mucin

Interactions of the hydrogels with mucin were evaluated through changes in viscosity after diluting the hydrogels to the half with the mucin solution (5 % final concentration) [73]. After vigorous stirring for 2 h, all formulations combined with mucin presented higher viscosity than the hydrogels without mucin (Fig. 7). This was mainly observed for the CMC + PVA gels. For the gellan gum formulation containing nano-papain, the viscosity of the mixture with mucin at a low shear rate was lower than the one observed for the gel alone. However, at higher shear rates, the mixture containing mucin presented higher viscosity.

The viscosity coefficient and the force of bioadhesion of the mixtures with mucin were analyzed using Eqs. (2) and (3), respectively [74], and the results are summarized in Table 2.

$$\eta_t = \eta_m + \eta_p + \eta_b \quad (2)$$

$$F_b = \eta_b \, \gamma \quad (3)$$

In these equations, η_t is the viscosity coefficient of the system (Pa·s); η_m = individual viscosity coefficient of mucin (Pa·s); η_p = individual viscosity coefficient of bioadhesive polymer (Pa·s); η_b = viscosity component due to bioadhesion (Pa·s); F_b = force of bioadhesion (Pa); γ = shear rate (s^{-1}) at which the viscosity value was calculated.

The viscosity component due to bioadhesion (η_b) found for the

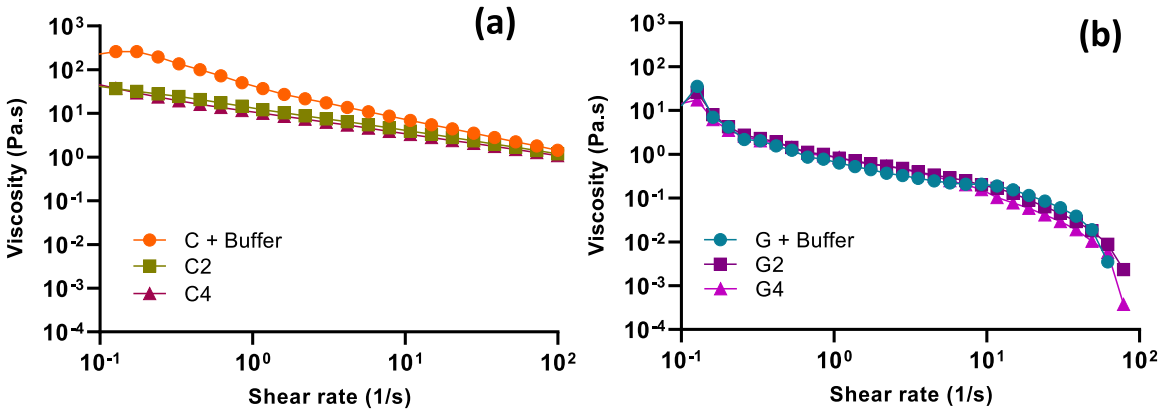

Fig. 6. Viscosity of (a) CMC + PVA formulations and (b) gellan gum formulations at 37 °C. Codes as in Table 1.

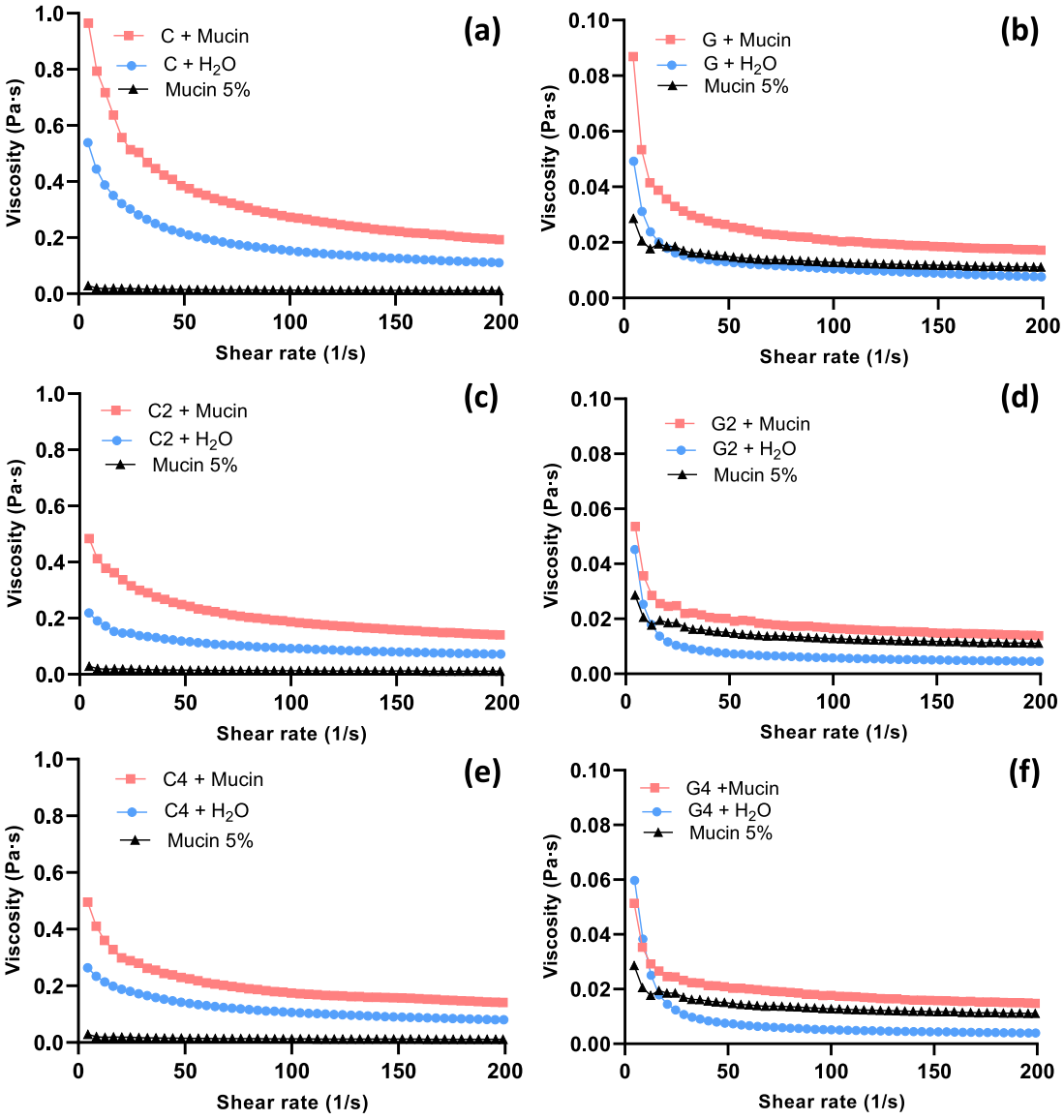

Fig. 7. Viscosity values recorded for mucin 5 % dispersion, mixtures of the hydrogels with mucin, and hydrogels mixed with buffer without mucin. (a) PVA + CMC; (b) gellan gum; (c) PVA + CMC with native papain; (d) gellan gum with native papain; (e) (CMC + PVA) + nanopapain; (f) gellan gum + nanopapain. Codes as in Table 1.

Table 2
Viscosity parameters and force of bioadhesion (F_b) for each formulation calculated by applying Eqs. (3) and (4), for the shear rate value (γ in s^{-1}) indicated in parenthesis.

Formulations	η_t (Pa.s)	η_m (Pa.s)	η_p (Pa.s)	η_b (Pa.s)	F_b (Pa)
G + mucin	0.087 ($\gamma = 4.4$)	0.028 ($\gamma = 4.5$)	0.049 ($\gamma = 4.6$)	0.001 ($\gamma_M = 4.5$)	0.004
G2 + mucin	0.054 ($\gamma = 4.6$)	0.028 ($\gamma = 4.5$)	0.045 ($\gamma = 4.4$)	−0.020 ($\gamma_M = 4.5$)	−0.091
G4 + mucin	0.051 ($\gamma = 4.5$)	0.028 ($\gamma = 4.5$)	0.060 ($\gamma = 4.7$)	−0.037 ($\gamma_M = 4.6$)	−0.170
C + mucin	0.965 ($\gamma = 4.6$)	0.028 ($\gamma = 4.5$)	0.539 ($\gamma = 4.4$)	0.398 ($\gamma_M = 4.5$)	1.790
C2 + mucin	0.483 ($\gamma = 4.4$)	0.028 ($\gamma = 4.5$)	0.219 ($\gamma = 4.4$)	0.236 ($\gamma_M = 4.4$)	1.038
C4 + mucin	0.495 ($\gamma = 4.4$)	0.028 ($\gamma = 4.5$)	0.264 ($\gamma = 4.4$)	0.202 ($\gamma_M = 4.4$)	0.890

mixture of gellan gum with mucin was low, but still positive, confirming a synergic effect between the two components. Similar findings were reported by Tayel and coworkers who developed nanoemulsion gels made of gellan gum for ophthalmologic applications and also reported mucoadhesion properties due to the synergism between gellan gum and mucin in rheological experiments, suggesting the formation of molecular entanglements and secondary chemical bonds between their formulation and the mucin glycoproteins [74]. Differently, a negative synergic effect was found with the decrease of the viscosity for the formulations of gellan gum containing papain, both in native and nanoparticulated form, probably due to the mucolytic action of the enzyme.

CMC + PVA hydrogels showed positive and higher bioadhesion components, in good agreement with previous reports [75]. The formulation without enzyme presented a η_b almost two times higher than the one found for the formulation containing nanopapain. CMC + PVA gels showed higher viscosity than gellan gum gels. This feature together with a higher content in polymers may explain why the presence of the papain did not lead to negative values in the interaction as observed in gellan experiments. Nevertheless, the significant decrease of η_b suggests that papain was also consuming the glycoproteins present in the mucin. Overall, these findings confirm the mucoadhesive behavior of the gels and papain mucolytic action, which may be important to increase the residence time of the formulation and the penetration thereafter of gemcitabine.

3.6. Hydrogels retention on bladder tissue

This assay was aimed to evaluate the *ex vivo* retention capacity of the formulations on bladder tissue after successive washes with artificial urine. The porcine bladder pieces were visualized in a fluorescence microscope under green light excitation (Fig. 8a). All gels had higher bioadhesion capacity than the control (FITC solution), especially after the thirdwash (15 mL). The gellan gum gels showed better mucoadhesion compared to CMC + PVA, showing higher fluorescence emission and apparent uniformity even after the fifth wash. It should be noted that this *ex vivo* test was carried out with the hydrogels without previous dilution, and therefore the more viscoelastic gellan gum hydrogels (Fig. 5) may withstand better the stress of the washing out. A published study about fluid gels for nasal drug delivery revealed that high acyl gellan gum was capable to prolong the release of the active substance for a longer period than the low acyl polymer, indicating better mucoadhesion properties of the first one [76]. The pH 6.2 of artificial urine was higher than gellan gum and mucin pKa (3.5 and 2.6, respectively) which caused the ionization of both substances. The negative charges would cause electrostatic repulsion followed by the expansion of polymeric matrix. Such expansion would facilitate the interpenetration of the polymer into the glycoproteins chains and engender supramolecular interactions between them [77,78].

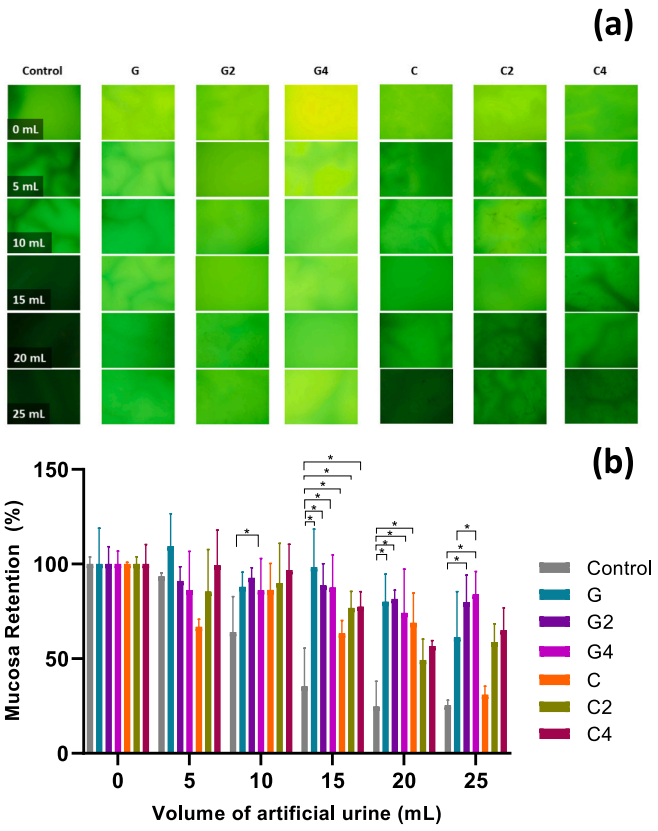

Fig. 8. (a) Fluorescence images of bladder tissues (green light excitation) once the hydrogels were applied on the surface and after successive washings with artificial urine and (b) Mucosa retention by means of fluorescence intensity - * indicates statistical significance ($p < 0.050$) . Codes as in Table 1.

The presence of papain also had some positive influence on the adhesion of the formulations. For the gellan gels, the nanoparticulate form seemed to be more efficient presenting difference with statistical significance between G formulation and G4 formulation on the last wash (25 mL) – Fig. 8b.

Papain may have helped in the interpenetration of the formulations with the mucin layer of the tissue, hindering the washing out. In previous reports using a similar setup, high molecular weight chitosan dispersions resisted up to 5 cycles of 10 mL washes [16]. Relevantly, the bladder retention of CMC grafted with graphene oxide was shown higher with the need of 200 mL of artificial urine for complete washing off of the formulation [24].

3.7. Bioadhesion strength

The bioadhesion strength test was performed on the formulations without the presence of the drug to gain further insight into the effects of papain on the bioadhesive properties. For this experiment, two portions of bladder tissue were arranged with their respective urothelium "face to face" and the formulation was placed in between. As a control, the same volume of 50 mM phosphate buffer was used instead of the hydrogels. The maximal force of detachment was used as an index of the force required to break the adhesive bonds formed between the formulation and the mucin present in the bladder tissue. The area under the force-distance curve informed about the total work of adhesion [16]. Concerning force of detachment, the formulations required a slightly higher force than the control (0.058 N) (Fig. 9a), and no significant differences were observed among formulations ($p > 0.05$). In terms of work of adhesion (Fig. 9b), all formulations had values higher than those recorded for the control, with statistically significance differences for

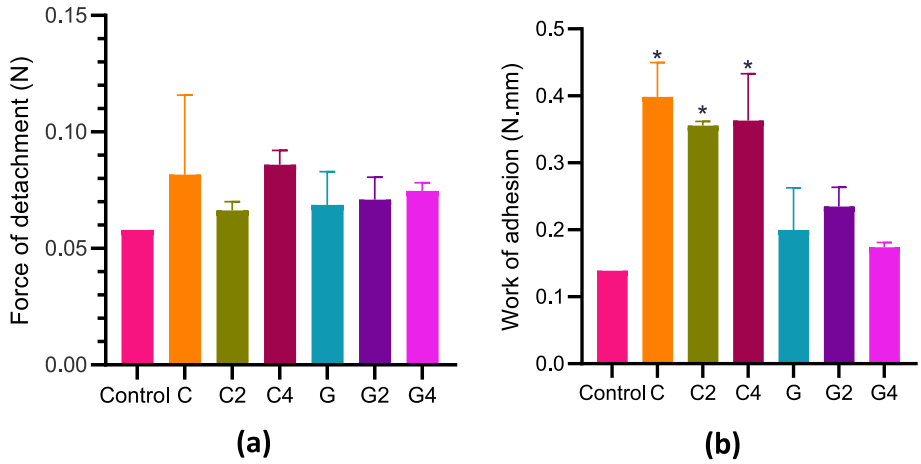

Fig. 9. Force of detachment (a) and work of adhesion (b) of the formulations tested in between two pieces of bladder tissue. 50 mM phosphate buffer was used as control. * The asterisk indicates statistically significant differences between referred formulation and control. Codes as in Table 1.

CMC + PVA formulations ($p < 0.05$), confirming that there were bioadhesive interactions between the bladder tissue and the gels.

These results were in good agreement with the results observed in Section 3.6 where the CMC + PVA formulations also presented higher bioadhesion components than gellan gum ones.

3.8. *In vitro* drug release

Once the formulation adheres to the urothelium, the sustained release of the chemotherapeutic agent for several hours may help to space out the bladder instillations. Sustained release of gemcitabine is expected to provide longer, more effective, and safer treatment. As shown in Fig. 10, the release of gemcitabine from the control (gemcitabine diluted in saline solution) was fast and 62.4 ± 11.7 % of the drug was delivered in the first 30 min of the test. Differently, both gellan gum and CMC + PVA formulations were able to provide a more sustained release during the first 6 h; the slowest values were recorded for CMC + PVA hydrogels which released only 13.8 ± 1.7 %, 8.5 ± 7.1 % and 9.5 ± 0.3 % of gemcitabine in the first 30 min, for formulations without enzyme (C1), with native papain (C3), and with nanopapain (C4), respectively. After 24 h, all CMC + PVA hydrogels had released all the loaded drug (98.8 ± 4.5 %; 101 ± 2 %; and 97.2 ± 1.5 %).

The results were in good agreement with those previously reported for physical gellan hydrogels loaded with B12 vitamin. A burst release of B12 vitamin (80 %) was observed in the first 8 h, even though their gellan matrices presented higher concentration (2 %) and the molecular weight of the solute was larger [79]. CMC and PVA films crosslinked with citric acid and loaded with water soluble drugs showed a release of 27 % of the drug (gentamicin sulfate) within the first hour followed by a released that lasted up to 8 h [80]. Our formulations presented a similar profile.

3.9. *Ex vivo* drug permeation

Ex vivo permeation assays were performed with the most promising formulations (CMC + PVA) considering their slower drug release profile, better mucoadhesive properties, and stability. A gemcitabine solution with the same concentration as in the hydrogels (10 mg/mL) was used as a control. The CMC + PVA formulation, without the presence of the permeation enhancer agent (papain), was also tested to evaluate if there was an effective action of the enzyme. The amount of gemcitabine permeated through the bladder tissue as well as the amount retained

Table 3
Lag time (h) and steady-state flow (μg/cm^2·h) of gemcitabine through the bladder tissue and mass retained in bladder tissue after 7 h of permeation assay. Formulation codes as in Table 1.

Formulation	Lag time (T_0 -h)_	Steady state flow (J - μg/cm^2·h)	Gemcitabine mass retained (μg)
Control	2.3 ± 0.2	60.5 ± 18.8	792.2 ± 9.4
C1	1.5 ± 0.3	10.8 ± 10.3	271.4 ± 4.3
C3	0.6 ± 0.6	24.3 ± 10.7	198.4 ± 14.8
C5	1.8 ± 0.03	23.6 ± 2.4	253.5 ± 6,2

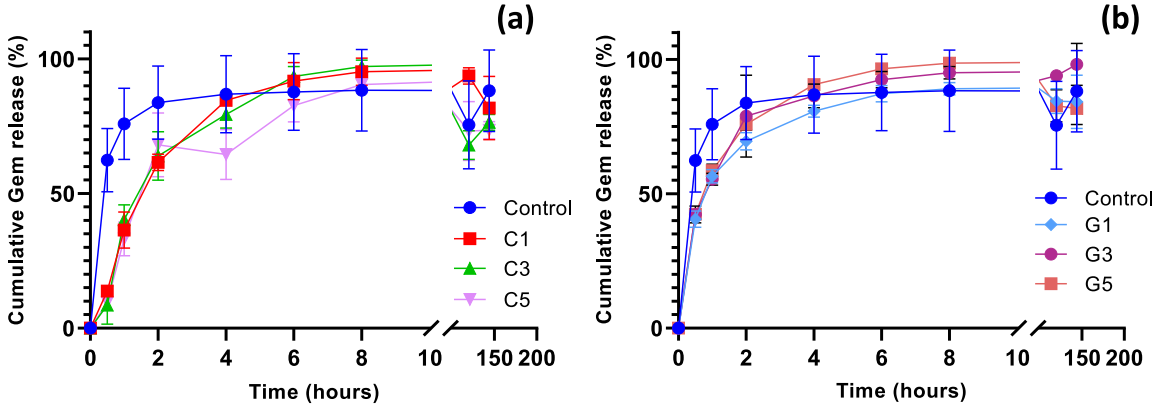

Fig. 10. *In vitro* cumulative release profiles of gemcitabine from (a) the CMC + PVA formulations and (b) gellan gum formulations. Mean values with standard deviations ($n = 3$). Codes as in Table 1.

were quantified by HPLC. The concentration of gemcitabine in the receptor chamber was quantifiable only after 2 h of experiment. The lag time decreased for CMC + PVA hydrogels with and without papain in comparison to the control (Table 3). At the timepoint of 2 h, the formulation containing papain presented a higher capacity of permeation as the values found were 13.6 ± 17.1 μg/cm^2, 8.6 ± 13.8 μg/cm^2, 43.8 ± 24.8 μg/cm^2, and 6.3 ± 3.0 μg/cm^2, for control, CMC + PVA without papain (C1), CMC + PVA with native enzyme (C3), and CMC + PVA with nanopapain (C5), respectively. However, through time, the controls presented a higher capacity of permeation, and therefore, higher concentration values in the receptor chamber were obtained (333.3 ± 114.4 μg/cm^2 at $t = 7$ h). This is probably due to the higher amount of gemcitabine free in the donor chamber since the very beginning for the control, while for the formulations, the gemcitabine is slowly released before permeating through the tissues. Formulation without enzyme (C1) presented the smaller concentrations for all the test period, with 63.45 ± 73.2 μg/cm^2 after 7 h. Differently, CMC + PVA with native papain (C3) was the formulation that exhibited the highest drug permeation capacity with 172.39 ± 57 μg/cm^2 (Fig. 11).

The lag time and steady-state flow calculated for the tested formulations are summarized in Table 3. The lag time was higher for the control when compared to the formulations containing hydrogel. Native papain seemed to fasten the time required for the drug to cross the tissue, as the decrease in lag time suggests that the hydrogel components promote the interaction of the drug with the urothelium. As previously verified in the rheological assay to evaluate formulations mucoadhesive properties, CMC + PVA hydrogels presented positive viscosity component due to bioadhesion, indicating the presence of physical and chemical bond energies in mucin-polymer interactions. The steady-state flux (J) values were in accordance with receptor chamber concentrations found, as control presented the highest one and CMC + PVA (C1) formulation the smallest value.

Concerning the mass retained in the bladder tissues (Table 3), the control free drug solution provided the higher amounts after 7 h test which can be related to higher and faster exposition of the tissue to the whole dose. Regarding CMC + PVA hydrogel formulations, all presented similar values of drug retained in the tissues, considering error. Overall, these results pointed out to the CMC + PVA hydrogel with papain (C3) as a suitable formulation to sustain drug release but facilitate drug penetration through the bladder mucosa.

3.10. Biocompatibility evaluation: cytotoxicity and HET-CAM assays

Cytotoxicity and HET-CAM assays were performed as a first screening of the cytocompatibility of the hydrogels without gemcitabine but with papain or nanopapain. Assays with HUVEC (human endothelial cell) cell line revealed that native papain either free or combined with gellan and CMC + PVA gels did not cause cytotoxicity, rendering cell viabilities higher than 70 % in all cases (Fig. 12). Differently, moderate toxicity was observed for nanoparticulated papain; both in its free form and in the gellan gum hydrogels the viability was below 75 %. Cell toxicity was not observed for the CMC + PVA gel with nanopapain and the apparent ability of the gel to stimulate cell proliferation was maintained.

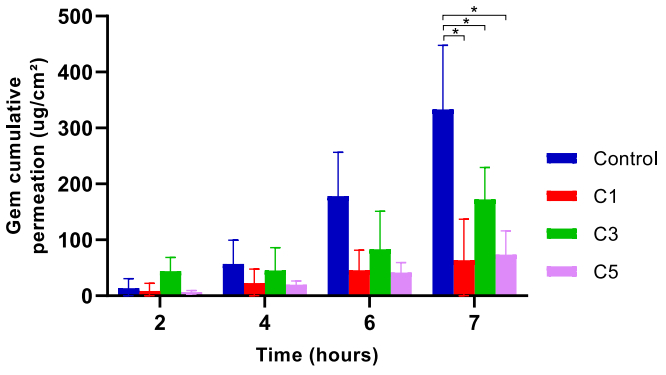

Fig. 11. Gemcitabine cumulative permeation through bladder tissue. The drug solubilized in saline solution was used as control. Codes as in Table 1.

For the V79–4 fibroblasts cell line, the hydrogels also showed no cytotoxicity. The fibroblasts showed higher sensitivity to papain, with cell viability <75 % for the native and nano papain either free or formulated in the gellan gum hydrogels. Differently, CMC + PVA hydrogels containing native or nano papain presented high cell viability.

In the assays with the HUVEC strain, only the gellan gum (G), gellan gum with nanopapain (G4), and CMC + PVA (C) formulations were statistically different from the negative control ($p < 0.05$). For the fibroblast cell line, native papain, nanopapain, gellan gum with native papain (G2), and gellan gum with nanopapain (G4), showed significant differences from the negative control ($p < 0.05$).

The HET-CAM is a simple and effective assay useful to predict the toxicity of formulations in a more *in vivo*-mimicking environment. The chorioallantoic membrane (CAM) of fertilized hen eggs is a complete laminate vascular tissue containing capillaries, veins, and arteries that can induce an inflammatory process in the presence of harmful agents. Therefore, it can be an easy and rapid way to screen formulations in terms of biocompatibility before pre-clinical and clinical studies [81,82] . As shown in Error! Reference source not found.S5, after 5 min in contact, all CAMs treated with formulations presented no visual signs of hemorrhage, lysis, or coagulation, suggesting that they are compatible with vascularized tissues.

4. Conclusion

Biocompatible polymers (Gellam gum, CMC, and PVA) already used for biomedical purposes and with interesting gelation properties were selected as vehicles for gemcitabine, an antitumoral drug widely used for bladder cancer treatment. As an innovative approach, papain was for the first time tested for this type of treatment as a permeability enhancer, to address the poor permeation of the tissue. The obtained results showed that our formulations presented pseudoplastic behavior and, therefore, suitable rheology for the proposed application, with the ability to be applied trough a syringe or catheter They were also demonstrated to have bladder bioadhesion capacity, with positive bioadhesion component and resistance to 5 cycles of synthetic urine washes. This feature is paramount as it could allow an extended residence time of the intravesical therapy. Gemcitabine release was prolonged for up to 24 h when loaded in the CMC + PVA blend. This could also provide a longer treatment and less frequent instillation protocol repetition, improving the compliance of the patient to the treatment. Moreover, papain mucolytic action was confirmed, as well as its capacity to improve the drug substance interpenetration across the bladder tissue when it was loaded in the gel, shortening the lag time to 0.6 h and doubling the amount of drug permeated in 7 h. These features of the formulations would have an extraordinary potential t to boost therapy by speeding up the chemotherapy absorption and preventing its loss in the urine.

The proposed formulations were also demonstrated to have great stability, being able to preserve up to 90 days papain proteolytic activity, for CMC + PVA blends, and to present low or no toxicity. Hence, they have great potential to move forward to preclinical studies and may represent a future upgraded alternative to intravesical therapy.

Therefore, in accordance with the above, the formulations developed here would represent a very notable improvement in clinical practice, ensuring a longer retention time of the formulation in the bladder tissue, avoiding its early elimination in the urine, and a more sustained release of the drug together with a greater permeation capacity and greater therapeutic compliance, which ultimately means less frequent instillations, greater patient compliance and therefore a reduction in both the social and health costs of the treatment.

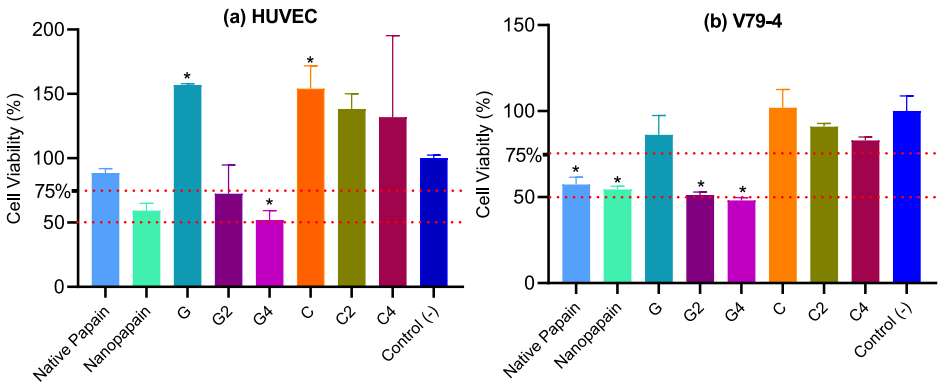

Fig. 12. Cell viability of (a) HUVEC and (b) V79–4 cell lines after incubation for 24 h with proposed formulations. Cells incubated with culture medium containing PBS instead of hydrogel were used as control (−). *The asterisk indicates statistically significant differences between referred formulation and control (−) ($p < 0.05$). Codes as in Table 1.

Funding

This research was funded by the São Paulo Research Foundation (FAPESP), grant number 2017/50332–0. The work was also partially funded by MCIN [Grant PID 2020–1184 113881RB-I00/AEI/10.13039/501100011033], Spain, FEDER and Xunta de Galicia [Grant ED431C 2020/17].

CRediT authorship contribution statement

Caroline S.A. de Lima: Conceptualization, Data curation, Formal analysis, Investigation, Methodology, Writing – original draft, Writing – review & editing. **M. Isabel Rial-Hermida:** Data curation, Formal analysis, Supervision, Writing – original draft, Writing – review & editing. **Lucas Freitas de Freitas:** Investigation, Data curation. **Ana F. Pereira-da-Mota:** Investigation, Data curation. **Maria Vivero-Lopez:** Investigation, Data curation, Writing – review & editing. **Aryel Heitor Ferreira:** Investigation. **Sławomir Kadłubowski:** Investigation. **Gustavo H.C. Varca:** Methodology, Supervision, Funding acquisition. **Ademar B. Lugão:** Supervision, Funding acquisition, Project administration, Resources. **Carmen Alvarez-Lorenzo:** Supervision, Investigation, Funding acquisition, Project administration, Resources, Writing – review & editing.

Declaration of competing interest

The authors declare that they have no known competing financial interests or personal relationships that could have appeared to influence the work reported in this paper.

Acknowledgments

C.S.A. acknowledges the São Paulo Research Foundation (FAPESP) for her PhD fellowships, grant numbers 2019/01315-1 and 2021/09636-1. M.I. R-H acknowledges Xunta de Galicia for her postdoctoral contract (ED481B 2018/009). A.F.P.-d.-M. is an ESR of the European Union's Horizon 2020 research and innovation program under Marie Skłodowska-Curie Actions Grant Agreement 813440 (ORBITAL).

Appendix A. Supplementary data

Supplementary data to this article can be found online at https://doi.org/10.1016/j.ijbiomac.2023.124957.

References

[1] F. Liedberg, et al., Local recurrence and progression of non-muscle-invasive bladder cancer in Sweden: a population-based follow-up study, Scand. J. Urol. 49 (4) (2015) 290–295, https://doi.org/10.3109/21681805.2014.1000963.
[2] T.C.M. Zuiverloon, et al., Recommendations for follow-up of muscle-invasive bladder cancer patients: a consensus by the international bladder cancer network, Urol. Oncol. Semin. Orig. Investig. 36 (9) (2018) 423–431, https://doi.org/10.1016/j.urolonc.2018.01.014.
[3] J.H. Buss, et al., Nano-BCG: a promising delivery system for treatment of human bladder cancer, Front. Pharmacol. 8, no. JAN (2018), https://doi.org/10.3389/fphar.2017.00977.
[4] E.J. Askeland, M.R. Newton, M.A. O'Donnell, Y. Luo, Bladder cancer immunotherapy: BCG and beyond, Adv. Urol. no. June (2012), https://doi.org/10.1155/2012/181987.
[5] P.V. Garcia, et al., Increased toll-like receptors and p53 levels regulate apoptosis and angiogenesis in non-muscle invasive bladder cancer: mechanism of action of P-MAPA biological response modifier, BMC Cancer 16 (1) (2016) 1–18, https://doi.org/10.1186/s12885-016-2474-z.
[6] F.G.E. Perabo, et al., Preclinical evaluation of superantigen (staphylococcal enterotoxin B) in the intravesical immunotherapy of superficial bladder cancer, Int. J. Cancer 115 (4) (2005) 591–598, https://doi.org/10.1002/ijc.20941.
[7] M.B. Oliveira, M. Villa Nova, M.L. Bruschi, A review of recent developments on micro/nanostructured pharmaceutical systems for intravesical therapy of the bladder cancer, Pharm. Dev. Technol. 23 (1) (2018) 1–12, https://doi.org/10.1080/10837450.2017.1312441.
[8] T.Y. Chen, M.J. Tsai, L.C. Chang, P.C. Wu, Co-delivery of cisplatin and gemcitabine via viscous nanoemulsion for potential synergistic intravesical chemotherapy, Pharmaceutics 12 (10) (2020) 1–11, https://doi.org/10.3390/pharmaceutics12100949.
[9] Y.T. Goo, et al., Optimization of a floating poloxamer 407-based hydrogel using the Box-Behnken design: in vitro characterization and in vivo buoyancy evaluation for intravesical instillation, Eur. J. Pharm. Sci. 163, no. April (2021), 105885, https://doi.org/10.1016/j.ejps.2021.105885.
[10] H.Y. Yoon, et al., Intravesical delivery of rapamycin via folate-modified liposomes dispersed in thermo-reversible hydrogel, Int. J. Nanomedicine 14 (2019) 6249–6268, https://doi.org/10.2147/IJN.S216432.
[11] P. Guo, et al., Intravesical in situ Immunostimulatory gel for triple therapy of bladder Cancer, ACS Appl. Mater. Interfaces 12 (49) (2020) 54367–54377, https://doi.org/10.1021/acsami.0c15176.
[12] O.M. Kolawole, W.M. Lau, H. Mostafid, V.V. Khutoryanskiy, Advances in intravesical drug delivery systems to treat bladder cancer, Int. J. Pharm. 532 (1) (2017) 105–117, https://doi.org/10.1016/j.ijpharm.2017.08.120.
[13] J. Yan, X. Chen, S. Yu, H. Zhou, Comparison of different in vitro mucoadhesion testing methods for hydrogels, J. Drug Deliv. Sci. Technol. 40 (2017) 157–163, https://doi.org/10.1016/j.jddst.2017.06.012.
[14] N.A. Peppas, J.J. Sahlin, Hydrogels as mucoadhesive and bioadhesive materials: a review, Biomaterials 17 (16) (1996) 1553–1561, https://doi.org/10.1016/0142-9612(95)00307-X.
[15] M.I. Rial-Hermida, A. Rey-Rico, B. Blanco-Fernandez, N. Carballo-Pedrares, E. M. Byrne, J.F. Mano, Recent Progress on polysaccharide-based hydrogels for controlled delivery of therapeutic biomolecules, ACS Biomater. Sci. Eng. 7 (2021) 4102–4127, https://doi.org/10.1021/acsbiomaterials.0c01784.
[16] O.M. Kolawole, W.M. Lau, V.V. Khutoryanskiy, Chitosan/β-glycerophosphate in situ gelling mucoadhesive systems for intravesical delivery of mitomycin-C, Int. J. Pharm. X vol. 1 (2019), https://doi.org/10.1016/j.ijpx.2019.100007. November 2018, p. 100007.
[17] J. Barthelmes, G. Perera, J. Hombach, S. Dünnhaupt, A. Bernkop-Schnürch, Development of a mucoadhesive nanoparticulate drug delivery system for a targeted drug release in the bladder, Int. J. Pharm. 416 (1) (2011) 339–345, https://doi.org/10.1016/j.ijpharm.2011.06.033.

[18] O.M. Kolawole, W.M. Lau, V.V. Khutoryanskiy, Methacrylated chitosan as a polymer with enhanced mucoadhesive properties for transmucosal drug delivery, Int. J. Pharm. 550 (1–2) (2018) 123–129, https://doi.org/10.1016/j.ijpharm.2018.08.034.
[19] D.B. Kaldybekov, S.K. Filippov, A. Radulescu, V.V. Khutoryanskiy, Maleimide-functionalised PLGA-PEG nanoparticles as mucoadhesive carriers for intravesical drug delivery, Eur. J. Pharm. Biopharm. 143 (July) (2019) 24–34, https://doi.org/10.1016/j.ejpb.2019.08.007.
[20] S. GuhaSarkar, P. More, R. Banerjee, Urothelium-adherent, ion-triggered liposome-in-gel system as a platform for intravesical drug delivery, J. Control. Release 245 (2017) 147–156, https://doi.org/10.1016/j.jconrel.2016.11.031.
[21] F. Yamamoto, R.L. Cunha, Acid gelation of gellan: effect of final pH and heat treatment conditions, Carbohydr. Polym. 68 (3) (2007) 517–527, https://doi.org/10.1016/j.carbpol.2006.11.009.
[22] K.M. Zia, et al., Recent trends on gellan gum blends with natural and synthetic polymers: a review, Int. J. Biol. Macromol. 109 (2018) 1068–1087, https://doi.org/10.1016/j.ijbiomac.2017.11.099.
[23] M. Kerec Kos, M. Bogataj, A. Mrhar, Mucoadhesion on urinary bladder mucosa: the influence of sodium, calcium, and magnesium ions, Pharmazie 65 (7) (2010) 505–509, https://doi.org/10.1691/ph.2010.9398.
[24] Y.Z. Low, L. Li, L.P. Tan, Investigating the behavior of Mucoadhesive polysaccharide-functionalized graphene oxide in bladder environment, ACS Appl. Bio Mater. 4 (1) (2021) 630–639, https://doi.org/10.1021/acsabm.0c01187.
[25] M. Burjak, M. Bogataj, M. Velnar, I. Grabnar, A. Mrhar, The study of drug release from microspheres adhered on pig vesical mucosa, Int. J. Pharm. 224 (1–2) (2001) 123–130, https://doi.org/10.1016/S0378-5173(01)00748-7.
[26] J.H. Chung, et al., The effects of hyaluronic acid and carboxymethylcellulose in preventing recurrence of urethral stricture after endoscopic internal urethrotomy: a multicenter, randomized controlled, single-blinded study, J. Endourol. 27 (6) (2013) 756–762, https://doi.org/10.1089/end.2012.0613.
[27] Y.C. Sim, et al., Stabilization of papain and lysozyme for application to cosmetic products, Biotechnol. Lett. 22 (2) (2000) 137–140, https://doi.org/10.1023/A:1005670323912.
[28] F.H. Arnold, Protein engineering for unusual environments, Curr. Opin. Biotechnol. 4 (4) (1993) 450–455, https://doi.org/10.1016/0958-1669(93)90011-K.
[29] K. Atacan, M. Özacar, M. Özacar, Investigation of antibacterial properties of novel papain immobilized on tannic acid modified ag/CuFe2O4 magnetic nanoparticles, Int. J. Biol. Macromol. 109 (2018) 720–731, https://doi.org/10.1016/j.ijbiomac.2017.12.066.
[30] F. Araújo, C. Martins, C. Azevedo, B. Sarmento, Chemical modification of drug molecules as strategy to reduce interactions with mucus, Adv. Drug Deliv. Rev. 124 (2018) 98–106, https://doi.org/10.1016/j.addr.2017.09.020.
[31] C. Menzel, A. Bernkop-Schnürch, Enzyme decorated drug carriers: targeted swords to cleave and overcome the mucus barrier, Adv. Drug Deliv. Rev. 124 (2018) 164–174, https://doi.org/10.1016/j.addr.2017.10.004.
[32] V.G. Tacias-Pascacio, et al., Immobilization of papain: a review, Int. J. Biol. Macromol. 188 (July) (2021) 94–113, https://doi.org/10.1016/j.ijbiomac.2021.08.016.
[33] N.F. Vasconcelos, et al., Papain immobilization on heterofunctional membrane bacterial cellulose as a potential strategy for the debridement of skin wounds, Int. J. Biol. Macromol. 165 (2020) 3065–3077, https://doi.org/10.1016/j.ijbiomac.2020.10.200.
[34] R.N.F. Moreira Filho, N.F. Vasconcelos, F.K. Andrade, M.F. de Rosa, R.S. Vieira, Papain immobilized on alginate membrane for wound dressing application, Colloids Surfaces B Biointerfaces 194, no. June (2020), 111222, https://doi.org/10.1016/j.colsurfb.2020.111222.
[35] FDA, Topical Drug Products Containing Papain v. 73, 2008.
[36] R. Chapman, M.H. Stenzel, All wrapped up: stabilization of enzymes within single enzyme nanoparticles, J. Am. Chem. Soc. (2019), https://doi.org/10.1021/jacs.8b10338.
[37] G.H.C. Varca, G.G. Perossi, M. Grasselli, A.B. Lugão, Radiation synthesized protein-based nanoparticles: a technique overview, Radiat. Phys. Chem. 105 (2014) 48–52, https://doi.org/10.1016/j.radphyschem.2014.05.020.
[38] G.H.C. Varca, S. Kadlubowski, M. Wolszczak, A.B. Lugão, J.M. Rosiak, P. Ulanski, Synthesis of papain nanoparticles by electron beam irradiation – a pathway for controlled enzyme crosslinking, Int. J. Biol. Macromol. 92 (2016) 654–659, https://doi.org/10.1016/j.ijbiomac.2016.07.070.
[39] G.N. Fazolin, G.H.C. Varca, S. Kadlubowski, S. Sowinski, A.B. Lugão, The effects of radiation and experimental conditions over papain nanoparticle formation: towards a new generation synthesis, Radiat. Phys. Chem. 169 (August) (2020), https://doi.org/10.1016/j.radphyschem.2018.08.033.
[40] G.N. Fazolin, G.H.C. Varca, L.F. de Freitas, B. Rokita, S. Kadlubowski, A.B. Lugão, Simultaneous intramolecular crosslinking and sterilization of papain nanoparticles by gamma radiation, Radiat. Phys. Chem. vol. 171 (2020), https://doi.org/10.1016/j.radphyschem.2020.108697 no. October 2018, p. 108697.
[41] B. Karavana, S.Y. Şenyiğit, Z.A. Çalışkan, Ç. Sevin, G. Özdemir, D.İ. Erzurumlu, Y. S. Şen, Gemcitabine hydrochloride microspheres used for intravesical treatment of superficial bladder cancer: a comprehensive in vitro/ex vivo/in vivo evaluation, Drug Des. Devel. Ther. 12 (2018) 1959–1975, doi: 10.2147%2FDDDT.S164704.
[42] C.C. Ferraz, G.H.C. Varca, M.M.D.C. Vila, P.S. Lopes, Validation of in vitro analytical method to measure papain activity in pharmaceutical formulations, Int J Pharm Pharm Sci 6 (Suppl. 2) (2014) 658–661.
[43] T. Eshel-Green, H. Bianco-Peled, Mucoadhesive acrylated block copolymers micelles for the delivery of hydrophobic drugs, Colloids Surfaces B Biointerfaces 139 (2016) 42–51, https://doi.org/10.1016/j.colsurfb.2015.11.044.
[44] S. Chutipongtanate, V. Thongboonkerd, Systematic comparisons of artificial urine formulas for in vitro cellular study, Anal. Biochem. 402 (1) (2010) 110–112, https://doi.org/10.1016/j.ab.2010.03.031.
[45] E. Caló, J.M.S.D. Barros, M. Fernández-Gutiérrez, J. San Román, L. Ballamy, V. V. Khutoryanskiy, Antimicrobial hydrogels based on autoclaved poly(vinyl alcohol) and poly(methyl vinyl ether-: alt -maleic anhydride) mixtures for wound care applications, RSC Adv. 6 (60) (2016) 55211–55219, https://doi.org/10.1039/c6ra08234c.
[46] M. N. Kirstein *et al.*, "High-performance liquid chromatographic method for the determination of gemcitabine and 2′,2′-difluorodeoxyuridine in plasma and tissue culture media," *J. Chromatogr. B Anal. Technol. Biomed.* Life Sci., vol. 835, no. 1–2, pp. 136–142, 2006, doi: https://doi.org/10.1016/j.jchromb.2006.03.023.
[47] S.Y. Karavana, et al., Gemcitabine hydrochloride microspheres used for intravesical treatment of superficial bladder cancer: a comprehensive in vitro/ex vivo/in vivo evaluation, Drug Des. Devel. Ther. 12 (2018) 1959–1975, https://doi.org/10.2147/DDDT.S164704.
[48] N. Toffoletto, A. Chauhan, C. Alvarez-Lorenzo, B. Saramago, A.P. Serro, Asymmetry in drug permeability through the cornea, Pharmaceutics 13 (5) (2021), https://doi.org/10.3390/pharmaceutics13050694.
[49] F. Alvarez-Rivera, D. Fernández-Villanueva, A. Concheiro, C. Alvarez-Lorenzo, α-Lipoic acid in Soluplus® polymeric Nanomicelles for ocular treatment of diabetes-associated corneal diseases, J. Pharm. Sci. 105 (9) (2016) 2855–2863, https://doi.org/10.1016/j.xphs.2016.03.006.
[50] S. Maiti, S. Jana, B. Laha, Cationic Polyelectrolyte–Biopolymer Complex Hydrogel Particles for Drug Delivery, Elsevier Inc., 2018.
[51] M.A. Morsi, A.H. Oraby, A.G. Elshahawy, R.M. Abd El-Hady, Preparation, structural analysis, morphological investigation and electrical properties of gold nanoparticles filled polyvinyl alcohol/carboxymethyl cellulose blend, J. Mater. Res. Technol. 8 (6) (2019) 5996–6010, https://doi.org/10.1016/j.jmrt.2019.09.074.
[52] C. Xiao, Y. Gao, Preparation and properties of physically crosslinked sodium Carboxymethylcellulose/poly(vinyl alcohol) complex hydrogels, J. Appl. Polym. Sci. 107 (2008) 1568–1572, https://doi.org/10.1002/app.27203.
[53] J. Milošević, B. Janković, R. Prodanović, N. Polović, Comparative stability of ficin and papain in acidic conditions and the presence of ethanol, Amino Acids 51 (5) (2019) 829–838, https://doi.org/10.1007/s00726-019-02724-3.
[54] G.F. Bickerstaff, H. Zhou, Protease activity and autodigestion (autolysis) assays using Coomassie blue dye binding, Anal. Biochem. 210 (1) (1993) 155–158, https://doi.org/10.1006/abio.1993.1166.
[55] S. Datta, L.R. Christena, Y.R.S. Rajaram, Enzyme immobilization: an overview on techniques and support materials, Biotech vol. 3 (1) (2013) 1–9, https://doi.org/10.1007/s13205-012-0071-7.
[56] W. Sheng, Y. Xi, L. Zhang, T. Ye, X. Zhao, Enhanced activity and stability of papain by covalent immobilization on porous magnetic nanoparticles, Int. J. Biol. Macromol. 114 (2018) 143–148, https://doi.org/10.1016/j.ijbiomac.2018.03.088.
[57] H. Dai, S. Ou, Z. Liu, H. Huang, Pineapple peel carboxymethyl cellulose/polyvinyl alcohol/mesoporous silica SBA-15 hydrogel composites for papain immobilization, Carbohydr. Polym. 169 (2017) 504–514, https://doi.org/10.1016/j.carbpol.2017.04.057.
[58] S.R. Sudhamani, M.S. Prasad, K. Udaya Sankar, DSC and FTIR studies on Gellan and polyvinyl alcohol (PVA) blend films, Food Hydrocoll. 17 (3) (2003) 245–250, https://doi.org/10.1016/S0268-005X(02)00057-7.
[59] K.R. Aadil, A. Nathani, C.S. Sharma, N. Lenka, P. Gupta, Investigation of poly (vinyl) alcohol-gellan gum based nanofiber as scaffolds for tissue engineering applications, J. Drug Deliv. Sci. Technol. vol. 54 (2019), https://doi.org/10.1016/j.jddst.2019.101276 no. September, p. 101276.
[60] X.J. Xu, et al., Effects of different acyl Gellan gums on the rheological properties and colloidal stability of blueberry cloudy juice, J. Food Sci. 83 (5) (2018) 1215–1220, https://doi.org/10.1111/1750-3841.14135.
[61] A.M.B.F. Soares, et al., Immobilization of papain enzyme on a hybrid support containing zinc oxide nanoparticles and chitosan for clinical applications, Carbohydr. Polym. 243 (May) (2020), https://doi.org/10.1016/j.carbpol.2020.116498.
[62] Z. Liu, D. Li, H. Dai, H. Huang, Preparation and characterization of papain embedded in magnetic cellulose hydrogels prepared from tea residue, J. Mol. Liq. 232 (2017) 449–456, https://doi.org/10.1016/j.molliq.2017.02.100.
[63] A.B. Nair, et al., Development of asialoglycoprotein receptor-targeted nanoparticles for selective delivery of gemcitabine to hepatocellular carcinoma, Molecules 24 (24) (2019), https://doi.org/10.3390/molecules24244566.
[64] D. Dutta, L.K. Nath, P. Chakraborty, D. Dutta, Targeting gemcitabine hydrochloride to tumor microenvironment through stimuli-responsive Nano-conjugate: synthesis, characterization, and in vitro assessment, J. Drug Deliv. Sci. Technol. vol. 60 (2020), https://doi.org/10.1016/j.jddst.2020.101981 no. June, p. 101981.
[65] N.F.A. Halim, S.R. Majid, A.K. Arof, F. Kajzar, A. Pawlicka, Gellan Gum-LiI gel polymer electrolytes, Mol. Cryst. Liq. Cryst. vol. 554 (2012) 232–238, https://doi.org/10.1080/15421406.2012.634344, no. December 2014.
[66] J. Zhu *et al.*, "Effect of Na2CO3 on the microstructure and macroscopic properties and mechanism analysis of PVA/CMC composite film," Polymers *(Basel)*., vol. 12, no. Cmc, pp. 1–13, 2020.
[67] O. Bird, R.B. Armstrong, R.C. Hassager, Dynamics of Polymeric Liquids. Volume 1: Fluid Mechanics, Wiley-Interscience Publication, John Wiley & Sons, New York, 1987.
[68] T.Z. Osmałek, A. Froelich, B. Jadach, M. Krakowski, Rheological investigation of high-acyl gellan gum hydrogel and its mixtures with simulated body fluids, J. Biomater. Appl. 32 (10) (2018) 1435–1449, https://doi.org/10.1177/0885328218762361.

[69] D. Kundu, T. Banerjee, Carboxymethyl cellulose-Xylan hydrogel: synthesis, characterization, and in vitro release of vitamin B 12, ACS Omega 4 (3) (2019) 4793–4803, https://doi.org/10.1021/acsomega.8b03671.
[70] A. Katoch, A.R. Choudhury, Understanding the rheology of novel guar-gellan gum composite hydrogels, Mater. Lett. 263 (2020), 127234, https://doi.org/10.1016/j.matlet.2019.127234.
[71] J. Yang, et al., Water induced shape memory and healing effects by introducing Carboxymethyl cellulose sodium into poly(vinyl alcohol), Ind. Eng. Chem. Res. 57 (44) (2018) 15046–15053, https://doi.org/10.1021/acs.iecr.8b03230.
[72] H.A. Shouket, et al., Study on industrial applications of papain: A succinct review, IOP Conf. Ser. Earth Environ. Sci. 614 (1) (2020), https://doi.org/10.1088/1755-1315/614/1/012171.
[73] J. Bassi da Silva, S.B.S. de Ferreira, O. de Freitas, M.L. Bruschi, A critical review about methodologies for the analysis of mucoadhesive properties of drug delivery systems, Drug Dev. Ind. Pharm. 43 (7) (2017) 1053–1070, https://doi.org/10.1080/03639045.2017.1294600.
[74] S.A. Tayel, M.A. El-Nabarawi, M.I. Tadros, W.H. Abd-Elsalam, Promising ion-sensitive in situ ocular nanoemulsion gels of terbinafine hydrochloride: design, in vitro characterization and in vivo estimation of the ocular irritation and drug pharmacokinetics in the aqueous humor of rabbits, Int. J. Pharm. 443 (1–2) (2013) 293–305, https://doi.org/10.1016/j.ijpharm.2012.12.049.
[75] D. Ivarsson, M. Wahlgren, Comparison of in vitro methods of measuring mucoadhesion: Ellipsometry, tensile strength and rheological measurements, Colloids Surfaces B Biointerfaces 92 (2012) 353–359, https://doi.org/10.1016/j.colsurfb.2011.12.020.
[76] M.H. Mahdi, B.R. Conway, A.M. Smith, Development of mucoadhesive sprayable gellan gum fluid gels, Int. J. Pharm. 488 (1–2) (2015) 12–19, https://doi.org/10.1016/j.ijpharm.2015.04.011.
[77] V.M.O. de Cardoso, M.P.D. Gremião, B.S.F. Cury, Mucin-polysaccharide interactions: a rheological approach to evaluate the effect of pH on the mucoadhesive properties, Int. J. Biol. Macromol. 149 (2020) 234–245, https://doi.org/10.1016/j.ijbiomac.2020.01.235.
[78] V.M.O. de Cardoso, et al., Design of mucoadhesive gellan gum and chitosan nanoparticles intended for colon-specific delivery of peptide drugs, Colloids Surfaces A Physicochem. Eng. Asp. 628 (July) (2021), https://doi.org/10.1016/j.colsurfa.2021.127321.
[79] P. Matricardi, C. Cencetti, R. Ria, F. Alhaique, T. Coviello, Preparation and characterization of novel Gellan gum hydrogels suitable for modified drug release, Molecules 14 (9) (2009) 3376–3391, https://doi.org/10.3390/molecules14093376.
[80] V.S. Ghorpade, R.J. Dias, K.K. Mali, S.I. Mulla, Citric acid crosslinked carboxymethylcellulose-polyvinyl alcohol hydrogel films for extended release of water soluble basic drugs, J. Drug Deliv. Sci. Technol. vol. 52 (2019) 421–430, https://doi.org/10.1016/j.jddst.2019.05.013, no. December 2018.
[81] W. Steiling, M. Bracher, P. Courtellemont, O. De Silva, The HET-CAM, a useful in vitro assay for assessing the eye irritation properties of cosmetic formulations and ingredients, Toxicol. Vitr. 13 (2) (1999) 375–384, https://doi.org/10.1016/S0887-2333(98)00091-5.
[82] A.M. Alambiaga-Caravaca, M.A. Calatayud-Pascual, V. Rodilla, A. Concheiro, A. López-Castellano, C. Alvarez-Lorenzo, Micelles of progesterone for topical eye administration: interspecies and intertissues differences in ex vivo ocular permeability, Pharmaceutics 12 (8) (2020) 1–18, https://doi.org/10.3390/pharmaceutics12080702.